The role of the PhoU protein in *Sinorhizobium meliloti*

The role of the PhoU protein in *Sinorhizobium meliloti*

By:

Harsh Sharthiya

A Thesis

Submitted to the School of Graduate Studies

in Partial Fulfillment of the Requirements

for the Degree

Master of Science

McMaster University

MASTER OF SCIENCE (2013)

TITLE: The role of the PhoU protein in *Sinorhizobium meliloti*

AUTHOR: Harsh Sharthiya

SUPERVISOR: Dr. T. M. Finan

NUMBER OF PAGES: VIII, 80

Abstract

Phosphate is of central importance in cellular metabolism and since bacteria are often exposed to various concentration of phosphorous in their environment, they have acquired various Pi transport systems for its uptake. *Sinorhizobium meliloti* has three Pi-uptake systems: a low affinity system encoded by *pap-pit* and two ABC type systems encoded by the *phnCDET* and *pstSCAB* operons. It is currently known that $PstSCAB_2$, a high affinity, high velocity transporter is induced under Pi limiting conditions and its transcription is controlled mainly in a PhoB-P dependent manner. During excess phosphate conditions, the negative regulation of the Pho regulon seems to involve $PstSCAB_2$ and PhoU. PhoU appears to be a negative regulator of the Pho regulon however; the mechanism by which PhoU accomplishes this task is currently unknown. In *Escherichia coli* and some other bacteria, mutations in *phoU* result in constitutive Pho regulon expression as do mutations in the *pstSCAB* genes. In order to address the function of PhoU in *Sinorhizobium meliloti*, we report the creation of a *Sinorhizobium meliloti ΔphoU* mutant strain. Results from the analysis of the *S. meliloti ΔphoU* strain suggest that this mutant behaves similarly to *E. coli phoU* mutant where one observes constitutive expression of the Pho regulon.

Acknowledgments

Firstly, I would like to thank Dr. Finan for giving me the opportunity of working in his laboratory and providing me with support and guidance for the last two years. I would also like to thank Dr. Morton, Dr. Zhang and Dr. Milunovic for their advice and guidance they provided. Finally, I would like to thank Sabeena Santhirakumaran, Mary Fernandes, George diCenzo, Guianeya Perez-Hernandez and other lab members for friendship, support and fun we all shared.

I would also like to thank, Morohoshi and colleagues for a gift of the *E. coli phoU* mutant (MT4 and MT29) strains.

Table of Contents

List of Figures

List of Tables

Introduction

Rhizobia

Rhizobia are root-nodule bacteria that have the ability of fixing atmospheric nitrogen (N_2) in symbiosis with legumes. This symbiotic relationship is based on the exchange of organic acids from host plant and differentiated N_2 fixing form of the bacteria, called bacteroids. The host plant is provided with ammonia by the bacteria. Most of the rhizobial symbiotic nitrogen fixing bacterial species belongs to the genera *Rhizobium, Mesorhizobium, Sinorhizobium, Bradyrhizobium* and *Azorhizobium*.

Sinorhizobium meliloti, the organism studied in this thesis, is a Gram-negative soil bacterium and a member of the family Rhizobiaceae in the alpha subdivision of the proteobacteria. *S. melioti* is capable of entering into a symbiotic relationship with plants belonging to the genera *Medicago, Melilotus,* and *Trigonella* (1). On the roots of these plants *S. meliloti* forms nodules within which the differentiated bacteriods reduce N_2 gas to ammonia.

Phosphate limitation

In biological systems phosphorus is important as it plays a key structural and regulatory role in many of the biological processes within an organism. The most notable biological function of phosphate (Pi) is in energy transfer (ATP/ADP and NADP/NAD) and it is present in nucleic acids and membrane phospholipids. In most soil and aquatic environments, soluble bioavailable phosphorus, especially inorganic Pi (PO_4^{3-}) is often present at growth-limiting concentrations (in the micromolar range) (2). Bacteria have the ability to change their metabolism in response to the amount of phosphorus available. The strategies employed by organisms to deal with phosphorus limitation include: more efficient uptake of phosphorus compounds into cells or decrease phosphorus use when synthesizing their biomolecules. Increased ability to acquire phosphorus from the environment involves the induction of various genes whose gene products are involved in the uptake and acquisition of different phosphorus sources. This includes the $PstSCAB_2$ high affinity, high velocity Pi transporter (3, 4), expression of periplasmic alkaline phosphatases PhoA and PhoX (5, 6), in addition to

organophosphates and phosphonates transporters (7–11). There are also processes to decrease phosphorus dependency including replacing the membrane phospholipids with phosphorus-free lipids(12, 13) and replacing phosphorylated periplasmic glucans with non-phosphorylated glucans (Zaheer and Finan, unpublished). The strategies employed by cells not only help decrease phosphorus requirements, but it also releases a phosphorus molecule from the degradation of the phosphorus compounds that can be used by the cell.

In *S. meliloti* P metabolism and the Pho regulon, has been the subject of several reports (3, 6, 13–19). In order to cope with various phosphorus conditions in soil, *S. meliloti* has acquired low and high-affinity phosphate transport systems which are activated based on the amount of phosphorus available in the environment. When *S. meliloti* cells are growing in the presence of excess Pi, the low affinity pap(OrfA)-pit transport system encoded on the chromosome is activated and the products of the *orfApap-pit* genes transport Pi into the cell (16). In contrast, when cells are growing in Pi limited conditions, the high affinity, high velocity ABC type transport systems $PstSCAB_2$ and PhoCDET, encoded on the chromosome and the pSymB megaplasmid respectively, are transcriptionally activated to transport Pi into the cell (3, 16). Besides the response to Pi starvation by activating transcription of genes involved in the transport and assimilation of Pi, *S. meliloti* also evolved a mechanism for conserving phosphorus sources. As mentioned above, it has been previously reported that *S. meliloti* replace their membrane phospholipids with nonphosphorus lipids upon growth in Pi limiting conditions. When Pi is limiting, an increase in sulpholipids, ornithine lipids and the *de novo* synthesis of diacylglyceryl trimethylhomoserine (DGTS) lipids was observed (12).

Genes and Proteins involved in Phosphate regulation

The phosphorus limitation response in microbes is mainly co-ordinated by two-component signal transduction systems, which consist of the protein pairs PhoB-PhoR in gram-negative bacteria (20) and PhoP-PhoR in gram-positive bacteria (21). All genes that are part of the “Pho regulon” are controlled though the activity of these systems. PhoR

is a member of the class I family of histidine kinases in which the site of phosphorylation is adjacent to the conserved catalytic region (22, 23). Based on comparing the amino acid sequences of *Escherichia coli* PhoR and EnvZ protein involved in the sensory response to changes in environmental osmolarity, a catalytic domain, ATP-binding domain, PAS domain and dimerization and histidine phosphorylation domain have been identified (Figure 1) (23). Additionally, unlike other histidine kinases, PhoR does not have a substantial periplasmic region, which is the site where signals from the environment are recognized (23). It was observed that PhoR contains an additional domain with high helical content which contains a central span of six positively charged residues. The function of this highly charged region is unknown, but its high positively charged density may allow it to play a role in stabilizing membrane interactions(23). On the other hand, the response regulator, PhoB contains three functional domains, an N-terminal domain that is responsible for its phosphorylation and a C-terminal domain that is responsible for its interaction with RNA polymerase and binding to the Pho Box (24).

Under phosphate limiting conditions, PhoR autophosphorylates and then acts as a kinase and phosphorylates PhoB (PhoP). Thereafter, phosphorylated PhoB (PhoB-P) binds specifically to conserved 22-nucleotide DNA sequence (Pho Box) within the target gene promoter region. The Pho box is composed of two eleven-base pair (bp) repeats where the first seven are highly conserved (CTGTCAT) followed by four less conserved AT rich base pair(25). This conserved region is recognized by the PhoB protein, if Pho box overlaps with -35 box of the promoter, binding of PhoB-P results in transcriptional activation. On the other hand, if PhoB-P binds to the Pho box located on the non-coding strand of the -10 box it would result in transcriptional repression(27-28, Zaheer and Finan, Unpublished).

Phosphate regulation by cross regulation

Besides its importance in activating the Pho regulon during Pi limiting conditions, PhoR also plays a role in preventing the activation of the Pho regulon during high Pi environments. PhoR achieves this by dephosphorylating PhoB by acting as a

phosphatase during growth in excess Pi, thus preventing the inappropriate activation of the Pho regulon(23, 28). PhoB can also be activated through PhoR independent mechanism such as cross regulation by nonpartner histidine kinases such as CreC (29, 30) or small molecule phosphoryl donor(s) such as acetyl phosphate, as seen in *E. coli* (31). The CreB/C two-component system is activated in *E. coli* when glycolyric carbon sources are being fermented(31, 32). It was suggested that the normal function of CreC is to monitor changes in carbon supply and the cross-talk with PhoB reflects similarities between CreC and PhoR such that both serve as Pi donor for PhoB. Furthermore, phosphorylation of PhoB by acetyl phosphate, involved in synthesis of ATP, has been observed(33).

Mechanistic aspects of ATP-binding cassette (ABC) systems

ATP-binding cassette systems form one of the largest protein superfamilies that are found in all kingdoms of life (34). ABC systems couple the energy of ATP hydrolysis to variety of essential biological phenomena including transmembrane (TM) transport, and also for non-transport related processes (35, 36). ABC systems can be divided into three main functional categories; I) Importer that mediate the uptake of nutrients, II) Exporters that are involved in the secretion of various molecules and III) systems which are involved in translation of mRNA and in DNA repair and are not involved in transport (37). ABC transporters consist of two transmembrane domains (TMDs) that form the translocation pathway and two nucleotide-binding domains (NBDs) that bind and hydrolyze ATP (Figure 2). Based on structural and biochemical evidence, all ABC transporters are believed to function by an “Alternate-Access” mode, with the translocation path shuttling between outward-facing and inward-facing conformation in response to substrate and ATP binding (38). The NBD is the conserved domain of ABC transporter that is attached to various TMDs. NBDs have two sub-domains, one similar to the functionally unrelated RecA protein, and another noted as a “helical sub-domain”. Within NBDs, there are numerous conserved sequence motifs with specific functions, however two are most important; the P-loops (Walker-A motifs) and the LSGGQ motif,

located in the RecA-like sub-domain and helical sub-domain respectively (39, 40). In a full transporter, the two NBDs assemble such that they form a shared interface that generates two ATP binding and hydrolysis sites between the P-loop of one NBD and the LSGGQ motif of the other. When ATP is bound, the interface closes and the nucleotide are sandwiched between the NBDs (Figure 3A) (40, 41). Based on studying ATP hydrolysis in several ABC transporters, it is believed that two molecules of ATP are consumed during each round of transport cycle (40).

By looking at the crystal structures of various full length ABC transporters, a reasonable mechanism for coupling ATP hydrolysis to transport is provided. This coupling requires the transmission of the molecular motion from the NBDs to the TMDs. This is achieved by the conserved α-helices called "coupling helices" which are observed in all reported crystal structures of TMDs (40). These coupling helices are presumed to interact with grooves formed at the boundaries of the two sub-domains of the NBDs. Therefore upon binding of ATP, the gap between the NBDs closes which brings the two coupling helices closer together. Subsequently, the TMDs flip from facing inward to facing outwards. This transport mechanism is common between both ABC importers and exporters (Figure 3B). Generally, all ABC transporters make use of this mechanism to expose the binding site of TMDs to the two opposite sides of the membrane to transport substrates across the bilayer. Although, the general coupling mechanism is conserved amongst different transporters, the folds of the TMDs are not, thus the ABC transporters are further divided into three classes; type I and II ABC importers and the ABC exporters.

Type I ABC importers mediate the uptake of various substrates such as ions, sugars and amino acids, with help of a specific binding proteins that deliver the substrate to the transporter (34, 40). An example of this type of transporter is the HisPQM system specific for histidine transport and the MalFGK system specific for maltose transport. Whereas the importers of type II aid in the uptake of metal chelates, which are usually larger than the substrates of type I ABC transporters, such as cobalamine (vitamin B_{12}) or haem (42). An example of this type of transporter is the

BtuCD transporter for vitamin B_{12}. Generally type I transporter have 10-12 TM helices in their core and tend to be smaller than type II transporter that contain 20 TM helices (34, 40, 42).

The Pst System

$PstSCAB_2$ (Phosphate Specific Transport) is a high affinity, high velocity Pi ABC-type transporter that consists of: a periplasmic phosphate binding protein (PstS), two transmembrane proteins (PstC and PstA), two ATPase proteins (PstB) and an accessory protein PhoU, whose functional activity is unclear (43). This system is induced during Pi limitation and its transcription is predominately controlled in a PhoB-P dependent manner (3, 44). In *S. meliloti*, $PstSCAB_2$ and PhoU are encoded in a single operon along with PhoB (*pstSCABphoUB*), which is located downstream of *phoR,* and is encoded in an operon by itself (3). As these genes are located very close to each other, it is possible that they play a role in common pathway. However, this organization of the *pstSCAB-phoU* and *phoR-phoB* is not conserved across species (Figure 4 & 5). In the gram-positive *Streptococcus pneumoniae* a two-component regulatory system, PnpR-PnpS, is located immediately upstream of the Pst system (*pstSCAB-phoU*). However unlike PhoR-PhoB, the PnpR-PnpS does not seem to be functionally associated with the Pst system (45). In *Bukholderia sp.* contains *pstSCAB* in sequence in the order similar to that of *E. coli.* Hence it is predicated that *pstSCAB* has the potential to take up Pi from its environment(46). In *Caulobacter crescentus*, the gene cluster of *phoR-pstCAB-phoU-phoB* is involved in the stalk elongation, cell division and phosphate regulation. Where the *pstCAB-phoU-phoB* genes are in one operon, however the *pstS* gene was far away from this gene cluster(47). In *Bacillus subtilis* the *pstSCAB* genes are transcribed from a single promoter and encode a Pi uptake system that is regulated by the PhoR-PhoP two-component system homologous to the PhoR-PhoB regulatory system. However the *phoU* gene is missing, while there are two copies of *pstB* genes (*pstB1* and *pstB2*) and the *pst* operon is not involved in Pi regulation(44). In *Pseudomonas aeruginosa*, the gene order of the phosphate-specific transport (*pst*) operon is *pstC-pstA-pstB*, and the *pstS*

gene is located far from this operon (48, 49). In *E. coli*, *pstSCAB-phoU* is in one operon, whereas the *phoR-phoB* is encoded in a separate, bicistronic operon (43, 50).

In the majority of the species observed, the Pho regulon genes are induced under Pi-limiting condition, however during excess phosphate conditions the negative regulation of the Pho regulon seems to involve $PstSCAB_2$ and PhoU. The regulatory role of $PstSCAB_2$ was recognized based on previous observations where mutations in any of the corresponding genes led to constitutive expression of the Pho regulon in addition to reducing or abolishing Pi transport via $PstSCAB_2$ (3, 51, 52). Additional studies with point mutations within the nucleotide binding domain of PstB affect both the phosphate transport and expression of the Pho regulon (53). Whereas, certain substitutions within the transmembrane domains of PstA and PstC affect only the phosphate transport but not the expression of Pho regulon (53). These results suggest that phosphate transport and the repression of the Pho regulon by the $PstSCAB_2$ may not be completely linked.

While PhoR-PhoB is responsible for coordinating the transcriptional response to Pi limitation, it is hypothesized that PhoR does not directly sense Pi concentration (54). Instead, it has been proposed that the high affinity, high velocity transporter $PstSCAB_2$, and its accessory protein PhoU, are involved in sensing Pi concentrations and relaying this message to PhoR. It is suggested that the *E. coli* PhoR appears to interact with the Pst transporter ($PstSCAB_2$-PhoU) (55). They suggest this interaction is between the PhoR cytosolic domain, that includes the PAS (Per-Arnt-Sim) domain and the PstB of the Pst transporter and/or PhoU (28)

Based on previous studies, it is believed that the role of $PstSCAB_2$ in the regulation of the Pho regulon is based on its ability to sense external phosphate concentrations (28). It is assumed that the PstS binding to $PstCAB_2$ results in a conformation change that results in the inhibition of the PhoR kinase activity by PhoU. Furthermore, it is assumed that the binding of PstS with $PstCAB_2$ is achieved only after Pi is bound to the PstS, which implies that the Pho regulon should only be repressed in presence of excess phosphate. Even though this model seems plausible, work from

other systems suggests that this might not be fully correct. In eukaryotic organism *Saccharomyces cerevisae*, the accumulation of intra-cellular orthophosphate represses the phosphate limitation response(56, 57). Moreover, previous work in *S. meliloti* shows that when it was grown on alternate phosphate source 2-aminoethylphosphonate (AEP) as the sole phosphate source, the pho regulon is not induced and also it had only a minimal effect on the $PstSCAB_2$ dependent Pi transport (3). Thus it seems improbable that the PstS binds to AEP and then represses the Pho regulon; instead it may be that the Pho regulon is repressed in response to an intra-cellular signal. Also the crystal structure of the maltose transporter in *E. coli*, $MalFGK_2$-MalE, was observed to exist in three conformations (38). One of the conformations requires binding of both the ATP and the periplasmic substrate binding protein (MalE). MalE can be bound or unbound to its substrate maltose, inducing a conformational change of the $MalFGK_2$ transporter complex. Therefore, it is possible that PstS may not require Pi in periplasm in order to bind the $PstCAB_2$ complex and cause a conformational change that inhibits the expression of the Pho regulon, similar to how MalE does not require maltose in order to bind $MalFGK_2$.

As mentioned earlier, $PstSCAB_2$ does not play a role in the regulation of the Pho regulon of *B.subtilis* and this is even more interesting as *B.subtilis* does not have a PhoU homolog (44, 58, 59). In *B.subtilis*, Pho regulon genes are controlled by three two-component signal transduction systems: PhoP-PhoR, ResD-ResE and a phosphorelay which leads to the phosphorylation of Spo0A (60). During Pi limiting conditions, the Pho regulon is induced by PhoP-PhoR, analogous to the Pho regulon regulators PhoB-PhoR of *E. coli* (60). In addition, the ResD (response regulator) and ResE (histidine kinase) that have significant sequence homology to PhoP and PhoR are involved in activation of the Pho regulon genes by regulating transcription of the *phoPR* operon (27). Also the transition state regulatory protein AbrB positively regulates the transcription of the *phoPR* operon. In contrast, Spo0A-P leads to negative regulation of the Pho regulon by negatively regulating the *resD* and *abrB* transcription and induces sporulation (60).

The accessory protein, PhoU is a negative regulator of the Pho regulon; however, the mechanism by which PhoU accomplishes this is currently unknown. Genetic studies of PhoU have shown that deletion of *phoU* leads to a severe growth defect, possibly due to accumulation of excess intra-cellular Pi by the functional $PstSCAB_2$ transporter in absence of PhoU (61). In *E. coli*, PhoU seems to play a role in controlling the activity of $PstSCAB_2$ transporter (55) but it is not required for the Pi transport via the $PstSCAB_2$ (61). Additionally, based on the phosphate uptake assay in *E. coli,* the absence of PhoU increases the rate of Pi uptake and the total Pi accumulated in the cells (55). As previously reported, PhoU deletions lead to constitutive expression of the Pho regulon in *E. coli* (62), therefore PhoU is required for the negative regulation of the Pho regulon and it has been suggested that this regulation is achieved by an interaction between PhoR and PhoU. In one study using FRET analysis no interaction between PhoR and PhoU was found; however, the experiment was carried out under Pi starvation, when PhoU does not repress the Pho regulon (63).

Crystal structures of PhoU

To gain additional understanding of the possible activity of the PhoU protein, we can look at the crystal structures of PhoU determined from four species: *Geobacillus stearothermophilus* (PDB: 1XWM) (Figure 6A), *Streptococcus pneumoniae* (PDB: 2I0M) (Figure 6B), *Aquifex aeolicus* (PDB: 1T72) (Figure 6C) and *Thermotoga maritime* (PDB: 1SUM) (Figure 6D). All of the four structures are highly similar, and each contains the basic PhoU topology consisting of six α-helices that are further organized into two PhoU domains each composed of three α-helix bundle. Analysis of the *A. aeolicus* PhoU crystal structure indicated possible metal-binding site in each domain (64). Furthermore, the crystal structure of *T. maritima* revealed two multinuclear metal cluster bounds to the protein surface: a tetranuclear iron cluster, which contains three irons, one nickel and a phosphite molecule bound to the N-terminal binding site and a trinuclear iron cluster containing three iron ions and a phosphite molecule bound to the C-terminal binding site (Figure 6E) (65). The presence of a phosphite in these structures perhaps suggests

that intra-cellular orthophosphate may control the activity of PhoU via a direct interaction in complex with metal ions. Based on a genetic approach to study structure-function relationship of PhoU in *E. coli*, it was observed that several point mutations, even within the highly conserved aspartic residue in the metal-binding site had only a slight decrease in its activity (55). Since PhoU is composed of two tandem three-helix bundles, it may be that there is a functional redundancy between the two halves of the protein (55).

Overall PhoU has no known structural analogs in the protein data base; however a single domain of PhoU has many matches (64, 65). The strongest structural similarity is to the Bcl2-associated anthanogene (Bag) domain found in Bag/Hsc70 complex, which is a cofactor of the eukaryotic heat shock protein Hsp70 family (64, 65). Interestingly, the ATPase domain of the Hsc70 has significant similarity with the histidine kinase domain of PhoR (64). Considering the Hsc70-PhoR and Bag-PhoU similarity, it is possible that PhoU plays a role in the PhoR-PhoB system similar to that of the Bag domain in the Hsc70-substrate complex, where PhoU may stimulate the dephosphorylation of PhoB by interacting with PhoR and PhoB-P (64).

Material and methods

Media and growth conditions

Luria-Bertani (LB; 10g/L tryptone, 5g/L yeast extract and 5g/L NaCl) broth was used for growth of *E. coli*, and for *S. meliloti* LB-broth was supplemented with 2.5mM $MgSO_4$ and 2.5mM $CaCl_2$ (LBmc). LB agar (LB broth with 15g L^{-1}agar) was used as a complex media for growth of both *E. coli* and *S. meliloti* on solid media. For growth on minimal media, M9 (21.1mM KH_2PO_4, 18.0mM NH_4Cl, 45.9mM Na_2HPO_4, 0.25mM $CaCl_2$, 8.2mM NaCl, 1mM $MgSO_4$, 1µg/ml biotin, 10ng/ml CoCl2) and MOPS-buffered (40mM MOPS, 2mM K_2HPO_4, 20mM NH_4Cl, 1.2mM $CaCl_2$, 100mM NaCl, 2mM $MgSO_4$, 0.5µg/ml biotin, 10ng/ml $CoCl_2$,1X trace elements (4.13 mM Na_2Mo_4, 3.48 mM H_3BO_3, 2 mM $CuSO_4$, 2.53 mM $MnCl_2$, 3.48 mM $ZnSO_4$, 26.9 mM Na_2EDTA and 5.45 mM NaFeEDTA) minimal media was used. Both M9 and MOPS media was supplied with 15mM glucose (M9-glucose) as carbon source. For solid minimum media 15g L^{-1} agar was added to M9 and MOPS buffered minimal media. When necessary, solid media were supplemented with appropriate antibiotics with final concentration as follows: 200µg ml^{-1} streptomycin (Sm), 200µg ml^{-1} neomycin (Nm), 60µg ml^{-1} gentamycin (Gm) and 5µg ml^{-1} tetracycline (Tc) for growth of *S. meliloti* and 100µg ml^{-1} ampicillin (Amp), 25µg ml^{-1} kanamycin (Km), 10µg ml^{-1} gentamycin (Gm) for *E. coli*. For all strains, antibiotic concentrations were halved for growth in liquid media. When included, the concentration of Isopropyl-B-D-1-thiogalactopyranoside (IPTG) was 0.5mM, 5-bromo-4-chloro-3-indolylphosphate (X-Phos) was 50mg L^{-1} and 5-bromo-4-chloro-idolyl-B-D-galactopyranoside (X-gal) was 40µg ml^{-1}. The X-Phos and X-gal was used for detection of bacterial alkaline phosphatase (BAP) and B-galactosidase, respectively.

Preparation of Genomic DNA

Rhizobia strains were inoculated in 5 mL of LB broth and grown overnight. All 5 mL culture was centrifuged and cell pellets were washed with 1 mL of 0.85% saline and resuspended in 600µl of $T_{10}E_{25}$ (10mM Tris, 25mM EDTA, pH 8.0) followed by addition of

SDS to 1%, Proteinase K to 0.5 mg/mL, and NaCl to 1 M. Samples were then mixed gently and incubated at 65^{o}C for 2 hours. DNA then was extracted with equal volume of Tris buffer-saturated phenol (pH 8.0) and twice with equal volume of phenol:chloroform (1:1) and once with 1 mL chloroform. The clean supernatant was then transferred to a new micro-centrifuge tube followed by addition of sodium acetate to 0.5M along with equal volume of isopropanol. The precipitated nucleic acid were spooled out using a pipette tip and placed in a new micro-centrifuge tube and washed with 70% ethanol followed by centrifugation. Pellet was dried by air after pouring out ethanol. The dried pellets were dissolved in 500µl of $T_{10}E_1$ (10mM Tris, 1mM EDTA, pH 8.0) with 20µg/mL RNaseA and incubated at 37^{o}C for 30 minutes. DNA was extracted once with equal volume of phenol:chloroform (1:1) and twice with equal volume of chloroform. Genomic DNA was precipitated, washed and dried as above. The dried pellets were resuspended in ddH_2O and 5µl was run on 0.8% agarose gel to determine quality and concentration of DNA.

Polymerase Chain Reaction (PCR)

All PCRs had a final volume of 25µl, consisting of 15ng of template DNA, 1x PCR HiFi buffer (Invitrogen), 200uM of dNTP mix (50µM dGTP, 50µM dATP, 50µM dTTP and 50µM dCTP), 0.3µM of each forward and reverse primers, 2mM $MgSO_4$ and 1.5U of HiFi *Taq* polymerase (Invitrogen). All reactions involved an initial denaturing step of 94^{o}C for 4 minutes, followed by 30 cycles of 60 second denaturing step at 94^{o}C, an annealing step (30 seconds) with temperature specific to set of primers used and extension step (72^{o}C) which varied in time depending on the specific reaction. Following the completion of 30 cycles, there was a final step of 10 minutes at 72^{o}C. All DNA segment amplified for cloning were performed six times in parallel reactions.

Agarose gel extraction

PCR products being used for ligation were extracted from agarose gel using QIAquick: Gel extraction kit (QIAGEN) and eluted in 90µl of elution buffer, whereas PCR products used for electroporation was eluted in 30-40µl of elution buffer.

Plasmid preparation

QIAprep spin Miniprep Kits (QIAGEN) was used to extract plasmids that were being checked for the correct insertion of the PCR product and the size of the plasmid. However, plasmids being used for ligation reaction were prepared using alkaline lysis.

Digestion

Plasmid and PCR product digestion were performed in a 50µl reaction. All digestion reactions contained 1X BSA (New England BioLabs), 1X the appropriate NEB buffer (New England BioLab), 10-20U of the appropriate restriction enzyme (New England BioLabs) and 8µl of plasmid DNA or 30µl of PCR product.

Alkaline Lysis

The overnight grown culture was spun down using centrifuge in a 1.5ml eppendorf tube. Bacterial cells were resuspended in 200µl of alkaline lysis buffer I (50mM glucose, 25mM Tris-HCl (pH 8), 10mM EDTA (pH 8)), then 400µl of alkaline lysis buffer II (0.2N NaOH and 1% W/V SDS) was added to the resuspended cells. Next 300µl of alkaline lysis buffer III (5M CH_3CO_2K) was added to the viscous bacterial lysate tube and stored on ice for 3-5 minutes. Thereafter, equal volume of phenol:choloroform (1:1 ratio) was added to the supernatant which is collected from centrifugation of cell lysate at 13000rpm for 2 minutes and mixed vigorously. Afterwards, the emulsion was centrifuged and the aqueous layer was collected, it was mixed with two-volumes of ice-cold 100% ethanol to precipitate nucleic acids from the supernatant. Precipitate was collected by centrifuging and was washed with 70% ethanol and was set to air dry, thereafter pellet was resuspended in appropriate volume of ddH_2O and stored in freezer.

Ligation

Ligation reactions were performed in 10µl of final volume. Ligation reaction contains 400U of T4 DNA ligase (New England BioLab), 5µl of digested PCR product, 3µl of digested vector and 1X ligation buffer (New England BioLab). Reaction was incubated at 16^oC overnight.

Gel Electrophoresis

Gel electrophoresis was performed using 0.8-1% agarose gel (containing 0.4µg/µl ethidium bromide) with final volume of 100ml. Samples were ran on the gel for approximately 1 hour and bands on the gel were visualized using UV light.

Transformation

The ligation mixture or plasmid DNA was added to 200µL of *E. coli* DH5α competent cells or appropriate recipient competent cells and incubated on ice for 30 minutes. Thereafter, cells were heat shocked at 42^{o}C in a water bath for 2 minutes and placed back on ice for 1 minute. Next 1 ml of LB was added to the transformation mixture and incubated at 37^{o}C for 1 hour 20 minutes. After incubation, the cell culture was centrifuged for 1 minute at 13000 rpm and 1 ml of LB was removed. The cell pellet was then resuspended in the remaining 200µl of LB supernatant, and all of the 200µl of cell culture was plated on appropriate selective media and incubated overnight at 37^{o}C.

Competent cells

Bacterial strains used to make competent cells were grown in 5ml culture overnight at 30^{o}C with agitation. The overnight culture was then subcultured into 100ml LB to an initial OD_{600} of 0.05 and was grown to final OD_{600} of 0.4. At this point, culture was transferred to two tubes of 50ml falcon tubes and was cooled down on ice for 15 minutes, after which it was centrifuged at 4^{o}C at 4500rpm and the cell pellet was collected. Next each cell pellet was resuspended in 25ml ice-cold 100mM $CaCl_2$ and was cooled on ice for 30 minutes. The resuspended cultures were once again centrifuged at 4^{o}C at 4500rpm and cell pellets were collected. These cell pellets were resuspended in 3ml of 100mM $CaCl_2$ containing 15% glycerol and were stored in -80^{o}C in aliquots of 200µl.

Electrocompetent cells

Bacterial strains used to make the electrocompetent cells were grown in 5ml culture with appropriate antibiotics overnight at 30^{o}C with agitation. This overnight culture was subculured in 100ml SOB buffer (2% Bactro Tryptone (Difco), 0.5% yeast

extract (Difco), 10mM NaCl, 2.5mM KCl, 10mM $MgCl_2$, 10mM $MgSO_4$ with 1mM L-arabinose) at 30^{o}C to an OD_{600} of 0.4. The culture was cooled down on ice for 15 minutes and then the cell pellet was collected by centrifuging the culture at 4^{o}C for 15 minutes. The cell pellet was resuspended and washed using 10% glycerol. Thereafter the culture was spun down and washed two more times, then the final cell pellet was resuspended in 3ml of 10% glycerol and was stored in -80^{o}C in aliquots of 75µl.

Alkaline phosphatase assay

From 3mL of overnight cultures grown, 1 mL of culture was washed and suspended in 1mL of LB media and OD_{600} was measured. To start the BAP (Bacterial alkaline phosphatase) reaction, 0.1mL of culture was mixed with 0.4mL of APX buffer containing 2mM para-nitrophenylphosphate (pNPP), 2mM $CaCl_2$ and 100mM Tris-HCl (pH 9.0). After incubation at room temperature, the reaction was terminated by the addition of 0.5mL of NaOH (0.5M). Then cells were pelleted, and the A_{410} of the supernatant was measured.

Conjugation

All conjugations in this study were carried out by using a helper *E. coli* strain MT616, carrying the pRK600 plasmid. The *E. coli* donor strain carrying the plasmid to be transferred, *S. meliloti* recipient strain and the helper MT616 strain were each inoculated in 5ml of LB or LBmc broth with appropriate antibiotics and grown overnight. 1mL of each culture was transferred to micro-centrifuge tube individually and was centrifuged. Cell pellets were washed with 1mL of 0.85% sterile saline three times and resuspended in 1mL saline. Subsequently, 50µl of each strain was mixed together in a micro-centrifuge tube and the full 150µl of mixture was spotted onto appropriate media plates (LB or MOPS) and allowed to grow overnight at 30^{o}C for plasmid transfer to occur. The overnight mating spot is collected and resuspended in 1mL sterile saline followed by preparation of serial dilutions ranging from 10^{0} to 10^{-6}. 100µl of each dilution is spread plated on appropriate plates for selection. Transconjugants are selected on media plates containing antibiotics for both the recipients and the plasmid being transferred, whereas

recipient are selected on plates containing antibiotics that allow growth of only the recipient strain. Then conjugation frequency is measured and the resulting colonies were streaked purified twice prior to use in further experiments.

SDS-PAGE and Western Blot

Proteins were separated by SDS-PAGE (Sodium dodecyl sulphate polyacrylamide) in gel casts and run in the Mini-PROTEAN Tetra cell (Bio-Rad) systems. Separating gels were made up of 375mM Tris (pH 8.8), 0.1% SDS, 10% Acrylamide bis (Bio-Rad), 0.05% APS and 0.01% TEMED and stacking gel was made up of 250mM Tris (pH 6.8), 10% Acrylamide bis, 0.1% SDS, 0.05% APS and 0.01% TEMED. 100 µl of 4X protein loading dye (250 mM Tris, 8% SDS, 0.04% bromophenol blue, 40% glycerol, 0.4M dithiothreitol) was added to a cell pellet of 1 mL culture at OD_{600} of 3.0 in a micro-centrifuge tube. The resulting mixture was boiled for 5 minutes and centrifuged. Then 7.5µl of supernatant was loaded onto a SDS-PAGE gel and ran at 150 volts for approximately 1 hour. Gels were stained overnight in Coomassie blue stain and destained using destaining solution (40% methanol, 10% acetic acid and 50% ddH_2O) until protein bands were visible.

For western blot analysis, the proteins were transferred from SDS-PAGE gels to PVDF membrane using the Trans-Blot SD Semi-Dry transfer cell system (Bio-Rad). The PVDF membrane was pretreated in 80% methanol for 1 minute and equilibrated in transfer buffer (48 mM Tris, 39 mM glycine and 20% methanol) for 5 minutes. A transfer sandwich of thick blotting paper, membrane, gel and another layer of blotting paper was made and placed in between transfer cell system. Transfer was run at 10 volts for 75 minutes. Thereafter, the membrane was carefully removed and was incubated in blocking buffer (5% skim milk) for 2 hours with shaking at room temperature. The membrane was then washed three times with 25 mL of TBST buffer for 10 min with shaking at room temperature. The membrane was treated with primary antibody overnight at $4^{o}C$ in 25 mL of TBST buffer containing 1.5% Skim milk and anti-PhoU and anti-DME serum (1:5000 fold dilution). Membrane was then washed three times with 25 mL of TBST buffer for 10 min and then was treated with secondary antibody for 2 hours

in 25 mL of TBST buffer containing 1.5% skim milk and goat anti-rabbit IgG-AP conjugate (1:3000 fold dilution) while shaking at room temperature. The membrane was then washed three times with 25 mL of TBST for 10 min with shaking at room temperature. Then membrane was exposed to Lumi-Phos WB chemiluminescent substrate for AP (Thermo-scientific) for 2 minutes and detection on alkaline phosphatase activity from AP-conjugated antibodies was performed using ChemiDoc MP imaging system (Bio-Rad).

Cloning of the S. meliloti phoR-pstSCAB-phoU-phoB region

In order to clone *S. meliloti phoR-pstSCAB-phoU-phoB* region on a plasmid, we employed deletion strategy using FRT targeting vectors pTH1522 and pTH1937. Using Rmfl5853 strain in fusion library strain constructed by vector pTH1522, which was used to construct a random insert library for the *S. meliloti* genome (66). Rmfl5853 strain has reporter gene *gusA* and *rfp* transcriptionally fused with *SMc02139* and *argD* genes located downstream of the *phoB* of the *pst* operon (Figure 7). Since plasmid pTH1522 carries a FRT site it was recombined into *S. meliloti* Rmfl5853 chromosome downstream of *pstSCAB-phoU-phoB* operon after the homologous recombination of the DNA fragment cloned in pTH1522 (66). Thereafter plasmid pTH2891 (pTH1937 carrying FRT site and homologous region to genes *SMc02148* located upstream of *phoR*) was recombined onto the chromosome of Rmfl5853 strain. This introduced another FRT site in Rmfl5853 strain located upstream of the *phoR* gene. Also between the two FRT site inserted, there are other genes of the plasmid pTH1522 and pTH2891 such as *oriT, nptII,* Gm^r, origin of replication (P15A and PMBI). Thereafter conjugation was performed between four strains MT616 (helper strain), Rmfl5853 strain with pTH1522 and pTH2891 recombined, M1449 strain carrying flp recombinase plasmid (pTH2505) and *E. coli* recipient (Rif^r) to capture the FRT-FLP recombinase mediated product. The

transconjugant (M2079) was selected on LB Rif and Gm plates and was patched to check Km resistance. Then transconjugant (M2079) was streaked purified on LB Rif and Gm plate and alkaline lysis was preformed to purify plasmid (pTH2892) DNA carried the *S. meliloti phoR-pstSCAB-phoU-phoB*.

Results and Discussion

S. meliloti phoU does not complement E. coli phoU mutants

Considering that the *E. coli* PhoU protein (241 amino acids) has 35% sequence identity and 66% sequence similarity to the *S. meliloti* PhoU protein (237 amino acids), it would seem likely that these two proteins have similar functions (Figure 8). Therefore, we investigated whether *E. coli pho*U mutants (*E. coli* MT4 and MT29) could be complemented with the *S. meliloti phoU* gene. In *E. coli* MT4 the 29th codon of the *phoU* gene is changed from glycine to aspartic acid, whereas in *E. coli* MT29 the 83rd codon of *phoU* is changed from an alanine to a threonine (67). The *E. coli* MT4 and MT29 mutants are known to accumulate large amounts of polyP, approximately 100nmol of Pi residues/mg of protein (100-fold higher than the wildtype strain, *E. coli* MG1655) due to the constitutive expression of *pstSCAB* (67). They also form blue colonies on agar containing X-Phos, as they constitutively express *phoA* encoding alkaline phosphatase (67). The chromogenic substrate 5-bromo-4-chloro-3-indolyl phosphate (X-Phos) is cleaved by alkaline phosphatase that produces a blue colored precipitate and colony which indicates presence of alkaline phosphatase activity (67).

In order to perform the complementation experiment with the *S. meliloti* PhoU we needed a positive control which would complement the phenotypes observed of the MT4 and MT29 mutant strains back to wildtype (approximately 1nmol of Pi residue/mg of protein and formation of white colonies on media containing X-Phos) thus allowing us to verify successful complementation results. The plasmid pMW*phoU* (*E. coli phoU* in

pMW119) was used as a positive control as it was previously reported to fully complement the MT4 and MT29 mutant phenotypes back to wildtype (67). Once the MG1655 (*E. coli* wildtype), MT4 and MT29 strains were successfully transformed with pMW119, pMWphoU, and pTH2887 (pMW119 plasmid carrying *S. meliloti phoU*), plasmids and were verified by isolating the plasmids from each strain and performing a restriction enzyme digest. A single colony from each transformation was streaked onto LB Amp plates containing X-phos, and the level of alkaline phosphatase expression was determined based on the formation of blue colonies (Table 2). The wildtype strain, MG1655 formed white colonies in all cases with or without any of the plasmid transformed. Both mutant strains MT4 and MT29 formed white colonies upon complementation with the pMW*phoU* plasmid, whereas transformation with pMW119 and the pTH2887 plasmids still formed blue colonies. These results suggest that *S. meliloti* PhoU was unable to complement the alkaline phosphate constitutive phenotype observed in the MT4 and MT29 *E. coli* PhoU mutant strains.

E. coli MT4 and MT29 strains were further used for alkaline phosphatase assays, in which para-nitrophenylphosphate (pNPP) is hydrolyzed by alkaline phosphatase to P-nitrophenol, forming a yellow colour. The level of alkaline phosphatase activity was determined based on the absorbance reading at 410nm (Figure 8). MT4 and MT29 with and without the empty pMW119 plasmid expressed high alkaline phosphatase activity. The MT4 and MT29 strains carrying the *E. coli* PhoU plasmid, pMW*phoU* expressed low alkaline phosphatase activity similar to the wildtype MG1655 strain. This was expected

since the plasmid pMW*phoU* was reported to complement the constitutive alkaline phosphatase activity phenotype of the MT4 and MT29 mutant strains (67). The MT4 and MT29 strains transformed with the plasmid, pTH2877 carrying *S. meliloti* PhoU had alkaline phosphatase activity in between the values measured for untransformed mutant strains and the mutant strains complemented by the *E. coli* PhoU. This was unexpected since MT4 (pTH2887) and MT29 (pTH2887) transformants produced blue colonies like the untransformed mutant strains on LB plates containing X-phos. The decreased alkaline phosphatase activity observed in this assay with the pTH2887 transformed strains suggests that the *S. meliloti* PhoU was partially able to complement the *E. coli* PhoU mutants MT4 and MT29, but not back to wildtype levels. The discrepancy between the two experiments could be explained by the fact that observing blue colonies on plate just indicates presence of alkaline phosphatase activity however it does not quantitatively measure its activity. Therefore if alkaline phosphatase is expressed even in a small quantity it will cleave X-Phos and form blue colonies. In comparison, the alkaline phosphatase assay allows to quantify the amount of activity present.

Construction of an S. meliloti ΔphoU gene mutant on Luria-Bertani (LB) media

To delete the *S. meliloti phoU* from the chromosome, we adapted Datsenko and Wanner λ Red-mediated recombination procedure designed for *E. coli* to replace the *phoU* gene with a Km^r cassette flanked by FRT sites (68) . This method allows us to make both polar and non-polar mutation for any gene(s). The *S. meliloti phoU* to be

inactivated was targeted using PCR product generated by PKD13-KanF1 and PKD13-KanR1 primers. Each primer is comprised of 20-nt 3' ends for priming of upstream and downstream of the FRT sites (FLP-recognition target site) flanking the kanamycin resistance gene in pKD13 template plasmid and 50-nt 5' ends homologous to upstream and downstream chromosomal sequences of the *S. meliloti phoU* (Figure 10A). Thereafter, using electroporation, this PCR product was transformed into the M1420 strain carrying plasmids pKD46 and pTH2889 (Figure 10B). Thereafter, recombination between PCR product and suicide plasmid pTH2889 comprised of *S. meliloti phoU* flanked by 340bp upstream and 352bp downstream homologous gene sequence inserted into pUCP30T suicide vector, generated plasmid pTH2895 (Figure 10C). In plasmid pTH2895, the *phoU* was replaced with the kanamycin-cassette (mentioned above). This was accomplished using the λ Red- mediated recombination between the 50-nt homologous ends of the PCR product generated by using PKD13-KanF1 and PKD13-KanR1 primers and the homologous upstream and downstream sequence of the *S. meliloti phoU* on the pTH2889. Plasmid pTH2895 carries Km-cassette gene flanked by FRT sites and ~350bp homologous upstream and downstream region of *S. meliloti phoU*. The λ Red recombination genes used in recombination were introduced on an easily curable, low copy helper plasmid pKD46, where synthesis of these genes was under control of a L-arabinose inducible promoter.

Thereafter tri-parental conjugation was performed using DH5α cells containing pTH2895 plasmid as the donor, *S. meliloti* RmP110 wildtype strain as the recipient and *E.*

coli MT616 as a helper strain to mobilize the pTH2895 plasmid. Thereafter transconjugants were selected on LB plates containing Sm and Nm. Transconjugants were also checked for loss of Gm resistance by patching them onto LB Gm plates to verify loss of the suicide plasmid. 3% of the Nm^r transconjugants were Gm^s. The subsequent strain (RmP3198, *S. meliloti* Δ*phoU2*::Km; Sm^R/Nm^R and Gm^S) was streak purified twice on LB Sm/Nm prior to further use. In order to eliminate Nm resistance from RmP3198, we use FLP-FRT recombination which is a site-directed recombination method that allows us to manipulate organisms DNA (69). The FLP recombinase binds to the 13bp sequence (5'-GAAGTTCCTATTC-3') of the 34-bp FRT sequence (5'-GAAGTTCCTATTCTCTAGAAAGTATAGGAACTTC-3') and mediates recombination between two FRT sites (69). RmP3198 strain has two FRT sites flanking each side of the Km-cassette insertion, thus using FLP we aim to eliminate the antibiotic resistance. Therefore a second conjugation was performed using M1449 donor strain containing FLP recombinase plasmid (pTH2505) and MT616 helper strain and RmP3198.

Transconjugants were selected on LB SmTc. Thereafter, transconjugants were streak purified on LB SmTc plates. Since we were deleting *phoU* in *S. meliloti* we wanted to determine if it has the same phenotype as *E. coli* Δ*phoU* mutants. For that reason it was hypothesize that if transconjugants were screened for presence of alkaline phosphatase activity by streaking them onto LB plates containing X-Phos where growth of blue colonies was expected as a Δ*phoU* deletion would likely lead to constitutive expression of alkaline phosphatase as it occurs in *E. coli* (61). However, the observed

results were unexpected because growth of both blue and white colonies was observed. This result suggested perhaps the colony streaked has a mixture of both type of cells ones with loss of Km-cassette and ones that still possesses Km-cassette on the chromosome. Therefore, a blue colony was streaked onto a LB SmTc X-Phos plate, where once again growth of both blue and white colonies was detected. In order to verify that the Km-cassette deletion had been made, a colony PCR was performed on a blue colony with primers that bind specifically to the Km-cassette insertion and primers that bind to the upstream and downstream region of the *phoU*, which is replaced by Km-cassette (Figure 11). The colony PCR gave contradicting results, where both PCR products were observed for blue colony: I) 600bp PCR product that is generated only if Km-cassette has been eliminated and II) 2kb PCR product that is generated only if Km-cassette is present on the chromosome as seen in lanes 6, 7, 10 and 11 (Figure 12). Also, some of the blue colonies were patched onto LB Sm/Nm plate to determine if they are neomycin sensitive however all the colonies patched showed resistance to neomycin. This result along with colony PCR results suggest that the transconjugants from the conjugation had a mix of two cell types; one with Km-cassette eliminated and another with Km-cassette still present on the chromosome.

Due to uncertain results the conjugation was performed again, however this time the expression of FLP from pTH2505 was induced by addition of 2.5mM protocatechuic (PCA) acid to the LB Sm/Tc plates. The mating spots were plated on both LB Sm/Tc and LB Sm/Tc (2.5mM protocatechuic acid) (Table 3). In the wildtype *S. meliloti* RmP110, FLP

plasmid pTH2505 transconjugants were obtained at similar frequencies, 1.27 x 10^{-1} and 2.28 x 10^{-1} respectively on both media. In contrast, RmP3198 (*ΔphoU2*::Km) transconjugants occurred at different frequencies on both media, 3.63 x 10^{-2} and 8.91 x 10^{-6} respectively. The difference in frequency between the uninduced and induced pTH2505 mated into RmP3198 compared to the wildtype strain suggests the colonies observed are likely to be suppressor mutants. This is because of the low conjugation frequency suggests that most of the cells are not viable after inducing the deletion and the ones that grew seems like would have gained a compensatory mutation that would allow them to grow after the deletion. As found in *E. coli*, a *phoU* deletion leads to growth defect and compensatory mutations within *pstSCAB* or *phoBR* genes, relieved that growth defect and allowed the *phoU* deletion cells to grow (55, 61). A suppressor mutation in *phoB* would lead to shut down of the entire Pho regulon, whereas mutations in *pstSCAB* would lead to regulon being constitutively expressed but would have a nonfunctional $PstSCAB_2$ transporter. Therefore it is possible that the *S. meliloti phoU* mutant strain has acquired suppressor mutations that allow it to grow while PhoB is constitutively expressed.

Similarly, another conjugation was performed with RmP3198 (*ΔphoU2*::Km) using constitutively expressed FLP from plasmid pTH1944 from M842 strain showed conjugation frequency similar to the one for RmP3198 strain mated with induced pTH2505 plasmid (Table 3). Thus looking at all the results, we can conclude that we were able to generate a *S. meliloti ΔphoU2::Km*-cassette insertion mutant on LB media but

attempts to create a *S. meliloti* Δ*phoU* mutant likely selected for possible suppressors. This could be because the Km-cassette insertion causes a polar mutation and inhibits expression of the downstream *phoB* as previously shown with Tn5 insertion in *S. meliloti phoU* (Yuan's MSc thesis). Therefore, elimination of Km-cassette flanked by FRT sites by FLP recombinase causes a non-polar mutation (*phoU*$^{-}$ and *phoB*$^{+}$) that allows expression of the downstream *phoB* constitutively and this constitutive expression of PhoB causes Pho regulon genes such as *pstSCAB* to be constitutively expressed. Perhaps this constitutive expression of the $PstSCAB_2$ proteins causes large amount of Pi to be accumulated inside the cells which is detrimental for its growth. This has been previously reported in *E. coli* where *phoU* mutant led to high levels of accumulated polyP in *E. coli* by constitutive expression of Pi-specific transport $PstSCAB_2$ (67). Therefore it appears that a Δ*phoU* deletion on LB media is lethal when PhoB proteins are constitutively expressed.

Using a similar approach another independent *phoU* mutant, RmP3203 (*S. meliloti* truncated Δ*phoU3*::Km) strain was generated where first 9-bp and last 12-bp of *phoU* is flanking the Km-cassette. Also when RmP3203 strain was conjugated with M1449 and MT616 to eliminate Km-cassette, similar results were found to the RmP3198 (*ΔphoU2*::Km) strain. Where the conjugation frequency of uninduced pTH2505 (FLP-recombinase) was 7.78×10^{-3} and induced pTH2505 (FLP-recombinase) was 1.40×10^{-6}.

Construction of an S. meliloti ΔphoU mutant on MOPS- aminoethylphosphonate media

Since we were unable to generate the *S. meliloti ΔphoU* mutant expressing PhoB on LB media plates we repeated the FLP-recombinase conjugation using plasmid pTH2505 and plated onto MOPS- minimal media plates supplemented with 2mM AEP (2-Aminoethylphosphonate) as a phosphate source and 15mM glucose as carbon source. The AEP used as phosphate source is taken up and catabolized by its own independent transport system known as *phnWAY* locus whose products *phnW, phnY* and *phnA* are not regulated by PhoB (10). This could allow *S. meliloti phoU* deletion strains to grow as the constitutive expression of phoB should not affect the uptake of 2-AEP. After conjugation between RmP3198 (*ΔphoU2*::Km), MT616 and M1449 (pTH2505), transconjugants were isolated at a frequency of 1.55×10^{-2}. These were streak purified on MOPS-2mM AEP Sm/Tc plates and then were patched on MOPS-2mM AEP Sm/Nm plates to check for neomycin sensitivity. 13 of the 50 patched colonies showed neomycin sensitivity. Thereafter, neomycin sensitive transconjugants were streaked on MOPS-2mM AEP plates containing X-Phos. As mentioned above, we wanted to know whether the *S. meliloti phoU* deletion mutants would have same phenotype as a *E. coli phoU* mutant, that expresses alkaline phosphatase constitutively (55, 61). After streak purification of tranconjugants (RmP3197) on MOPS 2mM AEP Sm plate, colony PCR was performed to verify elimination of Km-cassette from the chromosome (Figure 13). PCR results confirmed that Km-cassette was eliminated and a *S. meliloti ΔphoU* strain (RmP3197; *ΔphoU1*) was generated on MOPS 2mM AEP media.

The *phoU* deletion region from RmP3197 (*ΔphoU1*) was amplified by PCR and was sequenced to verify deletion (Figure 14). The intergenic region between *pstB* and *phoB* has an 82-bp scar from FRT-FLP recombination. Also based on sequencing, we detected a cytosine "C" deletion in the intergenic region between *pstB* and *phoB* (Figure 14). The 1-nt deletion probably resulted from kanamycin-cassette PCR product generated from a primer (PKD13-KanR1) lacking an internal base. The 1-nt deletion arose most likely during its chemical synthesis of 70-nt long primer (68). However, the sequence verifies that *phoU* was deleted successfully.

Complementation of S. meliloti ΔphoU strain

Once RmP3197 (*ΔphoU1*) was purified, it was streaked on LB and MOPS 2mM AEP media with X-Phos. RmP3197 formed blue colonies and the wildtype *S. meliloti* formed white colonies. In order to perform a complementation experiment both the empty pTrc plasmid and pTH2888 (Figure 15), which is pTrc plasmid carrying *S. meliloti phoU,* was mated *into* both wildtype *S. meliloti* RmP110 and RmP3197 strains. Strains RmP2381 (*S. meliloti* RmP110 with pTrc), RmP3204 (*S. meliloti* RmP110 with pTH2888), RmP3211 (*ΔphoU1* with pTrc) and RmP3200 (*ΔphoU1* with pTH2888) were plated onto LB with X-Phos and MOPS 2mm AEP with X-Phos plates to determine if expressing wildtype PhoU in *trans* would complement the RmP3197 (*ΔphoU1*) mutant phenotype (Table 4). The wildtype *S. meliloti* RmP110 strain formed white colonies with or without empty pTrc plasmid and pTH2888 in both LB and MOPS 2mM AEP media containing X-Phos. Whereas the RmP3197 strain formed blue colonies with or without empty pTrc

plasmid and pTH2888, thus indicating alkaline phosphatase activity in both LB and MOPS 2mM AEP media with X-Phos. This suggest, that RmP3197 (Δ*phoU1* strain) expresses alkaline phosphatase activity constitutively that is not complemented by having PhoU expressed in *trans*.

Alkaline phosphatase assays were performed to quantify the alkaline phosphatase activity for each strain in MOPS-0.02mM Pi (LPi), MOPS-2mM Pi (HPi) and MOPS-2mM AEP (Figure 16). *S. meliloti* RmP110 wildtype showed high alkaline phosphatase activity in MOPS-LPi media, whereas in MOPS-AEP and MOPS-HPi media had very low amount of activity as expected. This is because *phoX* encodes for alkaline phosphatase protein which is regulated by PhoB. As mentioned above *phoB* is part of the *pstSCAB* operon and is induced under low Pi condition. *S. meliloti* RmP110 strain carrying empty pTrc plasmid and pTH2888, RmP2318 and RmP3204 respectively, showed similar alkaline phosphatase activity as RmP110 strain. Whereas the *phoU* mutants RmP3197 (*ΔphoU1*) and RmP3211 (*ΔphoU1* with empty pTrc plasmid) showed high alkaline phosphatase activity in all three conditions, with highest activity measured in MOPS-HPi. The activity of the two *phoU* mutants, RmP3197 (*ΔphoU1*) and RmP3211 (*ΔphoU1* with empty pTrc plasmid) was significantly higher than for wildtype RmP110 strain. The RmP3198 (*ΔphoU2*::Km) strain is presumably $PhoU^-$ and $PhoB^-$ showed very low activity in all three conditions. Whereas, RmP3200 (*ΔphoU1* with pTH2888) showed alkaline phosphatase activity in all three conditions. However it was lower than the RmP3197 (Δ*phoU1*) and RmP3211 (Δ*phoU1* with pTrc plasmid) strains but higher than

the wildtype strains. Likewise, RmP3205 (*ΔphoU4* with pTH2888) and RmP3206 (*ΔphoU5* with pTH2888) strains, where Km-cassette was eliminated using FRT-FLP recombinase system in presence of t*rans* PhoU, show similar alkaline phosphatase activity (explained further below). Based on these results, it seems that the expression of PhoU from plasmid pTH2888 partially complements the constitutive expression of alkaline phosphatase activity of the RmP3197 (*ΔphoU1*) by decreasing the alkaline phosphatase activity of the mutant. However this was not back to wildtype level. This is unexpected because the *phoU* was deleted in RmP3197 from the chromosome and it resulted in constitutive expression of alkaline phosphatase activity. However having PhoU present in *trans* did not complement the alkaline phosphatase activity of the mutant back to wildtype level. Since the Δ*phoU* deletion in RmP3197 causes *pstSCAB-phoB* to be constitutively expressed, we thought perhaps the amount of PhoU expressed from the plasmid is not enough to negatively regulate the expression of *pstSCAB-phoB* back to wildtype level. Therefore western blot was performed to verify expression of PhoU in both wildtype RmP110 and in *phoU* mutant strains.

Western blot and chemiluminescence was performed on samples grown in MOPS-AEP (2mM AEP), MOPS-LPi (0.02mM Pi) and MOPS-HPi (2mM Pi) media (Figure 17). RmP110 grown in LPi had the highest amount of PhoU present based on chemiluminescence quantification. It had 38 fold the amount of PhoU present in MOPS-HPi media. Whereas, RmP110 strain grown in MOPS-AEP is 3 fold higher than MOPS-HPi. These values were measured by first standardizing all the samples using DME as a

reference protein. Intensity measured for each PhoU protein band was quantified against the reference band. Thereafter, the ratios were calculated based on the intensity of the PhoU measured between different media. Furthermore, using Western blots, it was verified that RmP3197 (*ΔphoU1*) and RmP3211 (*ΔphoU1* with pTrc plasmid) did not express PhoU in any of the media examined (Figure 18). In addition, it was also confirmed that plasmid pTH2888 does express PhoU (Figure 19). However two bands were observed for PhoU band around ~27kDa and we do not have an explanation for the existence of the two bands of protein on the blot. A previous study looking at RhaU over expression in *R.leguminosarum* also saw a similar result where two bands of RhaU protein were observed on a SDS page gel and they did not also have an explanation for the presence of two bands (70). Also, using the nucleotide sequence of pTH2888 plasmid, we translated all three reading frames starting at its promoter to determine that only one protein is translated. Due to unclear Western blot where the reference protein DME was not accurately transferred to membrane, we were not able to quantify the amount of PhoU present in the complemented mutant stains compared to wildtype strain; however the chemiluminescence showed over expression of PhoU from plasmid pTH2888. These results, suggest that PhoU is expressed in *trans* and is not able to complement the alkaline phosphatase phenotype of RmP3197 (*ΔphoU1*) strain back to wildtype like. Perhaps the over expression of PhoU from pTH2888 plasmid could be having an effect on the complementation of *phoU* mutant. This could be further

investigated by controlling the expression of PhoU in *trans* by having a plasmid that can be induced by addition of substrate or reagent to growth media.

Comparing growth of S. meliloti ΔphoU strain to the wildtype

The growth of the *phoU* mutant strain RmP3197 (*ΔphoU1*) was compared to that of the wildtype strain. Initially the cultures were grown in MOPS 2mM AEP buffer with appropriate antibiotics (Sm for strains without plasmid and Spec for strains carrying empty or pTH2888 plasmid) and were subcultured into MOPS-LPi (0.02mM Pi), MOPS-HPi (2mM Pi), MOPS-AEP (2mM AEP) and M9 media (without antibiotics) for growth curve (Figure 20 A-D). The result indicate that *phoU* mutants RmP3197 (*ΔphoU1*) and RmP3211 (*ΔphoU1* with pTrc plasmid) grew better than the wildtype RmP110 strain in MOPS-LPi and MOPS-HPi media. However since the machine stopped working at 34 hours none of the strains reached stationary phase so we cannot compare the maximum OD_{600} reached. In MOPS-AEP media RmP3197 and RmP3211 grows better than RmP110 initially but they both reach similar stationary phase at 42 hours. In the M9 media, the RmP3197 and RmP3211 strains grew to a lower stationary phase than the RmP110 strain. The growth curve of the RmP3200 strain (Δ*phoU1* with pTH2888 plasmid) shows a similar growth pattern to the RmP110 strain. Therefore the Δ*phoU* mutant strain carrying the pTH2888 plasmid seems to complement the growth phenotype of the mutant back to wildtype. Furthermore, the excess amount of Pi present in M9 media (40mM) compared to MOPS-HPi (2mM) seems to effect the growth of the *phoU* mutant strains RmP3197 (*ΔphoU1*) and RmP3211 (*ΔphoU1* with pTrc). It seems that high Pi

concentration in M9 media does not allow these strains to grow better than the wildtype strain RmP110. *E. coli phoU* mutants grew poorly in media containing elevated levels of Pi, and it was speculated that elevated levels of intracellular Pi level have a toxic effect (55). However we cannot be sure that this is the case for *S. meliloti* strains RmP3197 (*ΔphoU1*), RmP3211 (*ΔphoU1* with pTrc) because the growth difference is compared between two different media and therefore we cannot be sure that the growth difference is solely due to difference in Pi concentration. In order to verify the observed growth difference these strains need to be grown in MOPS media with varying Pi concentration to determine if Pi has any effect on growth of these strains.

Eliminating the kanamycin-cassette in RmP3198 with phoU in trans (pTH2888)

Initially, we were able to generate a $phoU^-$ and $phoB^-$ *S. meliloti* strain RmP3198 (*ΔphoU2*::Km) by inserting a Km-cassette into the *phoU* region; however we were not able to eliminate the Km-cassette using the FRT-FLP recombinase system. As the excision of the Km/Nm cassette will generate a $phoU^-$ $phoB^+$ strain, it appears that expression of PhoB in the absence of PhoU is lethal and thus no viable colonies were recovered on LB media. Previously in *E. coli* when the kanamycin cassette was transduced to knockout chromosomal *phoU,* no Kan^R transductants were recovered (61). Therefore they made the recipient strain diploid in *phoU* by having *phoU* in *trans* on a plasmid, thereafter they were successfully able to delete chromosomal *phoU* (61). Therefore, we mated in plasmid pTH2888 (Figure 15) into RmP3198 (*ΔphoU2*::Km) thus having *phoU* presence in *trans*. When plasmid the Flp plasmid pTH2505 was introduced

into the resulting strain RmP3209 (*ΔphoU2*::Km with pTH2888), Nm-sensitive transconjugants were readily obtained on LB media. RmP3205 (*ΔphoU4* with pTH2888) was one such transconjugant. Compared to previous conjugation frequencies mentioned above 3.63×10^{-2} and 8.91×10^{-6} respectively for uninduced and induced, the frequency for *trans* PhoU conjugation (RmP3209, *ΔphoU2*::Km with pTH2888) are 1.12×10^{-1} and is 1.41×10^{-2} for uninduced and induced pTH2505 (Table 3). This suggests that most of the colonies after elimination of Km-cassette from chromosome are still viable by having PhoU being expressed in *trans*. When RmP3205 (*ΔphoU4* with pTH2888) strain was struck onto LB and MOPS 2mM AEP agar containing X-Phos, all colonies were blue in color. This was unexpected, since the RmP3205 *phoU* deletion still carried phoU in *trans* on the plasmid pTH2888. This result is similar to the one where RmP3197 (*ΔphoU1*) strain that was complemented with pTH2888 plasmid after Δ*phoU* deletion was made. Therefore based on the results obtained, the PhoU in *trans* is only able to partially complement the Δ*phoU* mutation in strains RmP3197 (*ΔphoU1*), RmP3205 (*ΔphoU4* with pTH2888) and RmP3206 (*ΔphoU5* with pTH2888). The plasmid copy of phoU may allow cells to grow by possibly regulating the activity of $PstSCAB_2$ transporter and preventing accumulation of polyP, however it is not able to fully repress the constitutive expression of PhoB thus they are still expressing alkaline phosphatase activity.

Similarly strain RmP3206 (*ΔphoU5* with pTH2888) was generated from RmP3203 (truncated Δ*phoU3*::Km) strain that was first conjugated with plasmid pTH2888 before

eliminating Km-cassette from the chromosome by having PhoU in *trans*. The frequency for this uninduced pTH2505 conjugation is $8.63x10^{-3}$ and induced pTH2505 conjugation is $2.85x10^{-3}$, similar to that of RmP3205 (*ΔphoU4* with pTH2888). Also strain RmP3206 showed similar alkaline phosphatase activity to RmP3205 (Figure 16).

SacB seletion to generate unmarked ΔphoU deletion

A different approach to the λ Red recombinase system was used to generate an independent S. *meliloti phoU* mutant allele to the RmP3197. This experiment was started by Zaheer where, plasmid pJQ200mp18 (71) with two PCR insertions (pTH2418) 1) from nucleotides: 570657-571588 from *S. meliloti* chromosome that includes whole *pstB*, the intergenic region between *pstB-phoU* and the first 30-nt of *phoU*. 2) From nucleotides: 572240-573078 from *S. meliloti* chromosome that includes the last 25-nt of *phoU*, the intergenic region between *phoU-phoB* and the whole *phoB* sequence (Figure 21A) was used. This plasmid was then recombined onto *S. meliloti* RmP110 chromosome via a single crossover recombination and transconjugants were selected on LB Sm/Gm. The two possible homologous recombination sites between the plasmid and chromosome are the two PCR inserts 1 and 2 on plasmid and its corresponding sequence on the chromosome (Figure 21B). Thereafter, double recombinants (*ΔphoU* strain (Figure 21C)) were selected on MOPS-2mM AEP (5% sucrose) with X-phos. This media was used because, plasmid pTH2418 carries *sacB*, which encodes for levansucrase and in presence of sucrose, levansucrase is lethal which causes cell lysis in gram-negative bacteria and this would allow a method for selection for loss of vector (71). Since Δ*phoU*

deletion produces blue colonies on media containing X-phos, transconjugants that were slightly blue/dark blue were then screened for loss of Gm^R and were streaked onto MOPS-2mM AEP media containing 5% sucrose. To investigate whether these colonies carried a *phoU* deletion, colony PCR was performed using primer set 1 (Pst-1937F and Pst-1937R) and primer set2 (DelphoUF and DelphoUR). Primer set 1 would generate a 600bp PCR product which would amplify upstream region of *phoR* and will be used as a positive control. Whereas primer set 2 will generate 750bp product if *phoU* deletion has been made, if not 1400bp product will amplified in strains where deletion is not made (Figure 22). RmP110 and all transconjugants had 600bp internal control gene amplified by primer set 1. As for the primer set 2 product, RmP110 along with all transconjugants had 1400bp product present along with one of the transconjugant also having 750bp product present. The transconjugant with both 750bp and 1400bp with primer set 2 was streak purified on MOPS 2mm-AEP with 5% sucrose plate and was checked for *phoU* deletion; however *phoU* was still present on the chromosome. Therefore, we can conclude that no unmarked Δ*phoU* mutants were recovered using *sacB* selection technique. This was unexpected since AEP is taken up and is converted to inorganic phosphate by gene locus *phnWAY,* which is not regulated by PhoB (10). As we know *phoU* mutation causes accumulation of polyP and leads to a growth defect in *E. coli* (55, 67). It is possible that in *S. meliloti* there is an unknown Pi exporter that exports excess internal Pi preventing accumulation of internal Pi. Where the activity of the exporter is negatively regulated by PhoB and since *phoU* mutation leads to constitutive expression

of PhoB, this would repress the activity of Pi exporter. Therefore uptake of AEP under constitutive PhoB expression could possibly lead to accumulation of internal Pi which can have a growth defect in *S. meliloti* and it maybe for this reason we were not able to generate any *S. meliloti ΔphoU* mutant using *sacB* selection. Based on the results from this experiment, it is possible that the Δ*phoU1* strain (RmP3197) isolated using λ Red recombinase system mentioned above on MOPS- 2mM AEP carries a second site suppressor mutation.

E. coli Phosphate uptake mutants

The plasmid pTH2892, containing *S. meliloti* PhoR-PstSCAB-PhoU-PhoB, was transformed into *E. coli* strains MG1655, MT2006 and MT2016. MG1655 is *E. coli* wildtype, MT2006 is a derivative of MG1655 that has all four phosphate transporters deleted (PitA, PitB, PhnCDE and $PstSCAB_2$) (72) . *E. coli* MT2016 is a MT2006 derivative in which three additional genes were deleted. These encode alkaline phosphatase (*phoA*), *yjbB* (contains PhoU and Na^+/Pi cotransporter domains) and the glycerol-3-phosphate transporter (*glpT*) (72) . Since MT2006 and MT2016 have all phosphate systems deleted, they cannot grow on inorganic phosphate as sole phosphorous source (72). However both strains MT2006 and MT2016 are able to grow in presence of glycerol-3-phosphate (G3P) using Ugp and/or GlpT transport systems (72). When the MG1655, MT2006 and MT2016 strains were transformed with pTH2892 were streaked, all three strains grew on M9 media containing mannitol, whereas the untransformed strains fail to grow. Therefore, the *S. meliloti* $PstSCAB_2$ transporter from pTH2892 allowed the *E. coli*

mutants to grow on M9 mannitol media. In addition, a growth curve was performed on these strains to see their growth compared to the wildtype (Figure 23). Based on the growth curve we can see that MT2006 and MT2016 grow relatively poorly compared to the wildtype strain MG1655 in M9 mannitol media. On the M9 mannitol media containing G3P the MT2006 and MT2016 strains grows similar to the MG1655 strain. MT2006 and MT2016 mutant strains carrying plasmid pTH2892 grows better than the mutant strains grown in M9 mannitol but poorer than the MG1655 strain. This suggests that $PstSCAB_2$ transporter of *S. meliloti* allows the *E. coli* mutants MT2006 and MT2016 to uptake phosphate on M9 mannitol media allowing them to grow.

Summary

The goal of this study was to generate *S. meliloti ΔphoU* deletion strains and determine if such mutants have a similar phenotype as *E. coli phoU* mutants. Firstly, we determine that *S. meliloti* PhoU was not able to completely complement *E. coli phoU* mutations in the MT4 and MT29 strains. We were able to generate PhoU$^-$ and PhoB$^-$ strain RmP3198, *S. meliloti ΔphoU2*::Km on LB media, however we were unable to generate a PhoU$^-$ and PhoB$^+$ *S. meliloti* strain on this media. Therefore a *S. meliloti* PhoU$^-$ and PhoB$^+$ strain was generated on MOPS-2mM AEP media. The *S. meliloti* Δ*phoU1* mutant strain (RmP3197) constitutively expressed alkaline phosphatase and presumably the Pho regulon. In *S. meliloti* strain RmP3197, the *S. meliloti ΔphoU* mutant phenotype was not fully complemented by expressing PhoU in *trans* from plasmid pTH2888, as it only partially reduced constitutive expression of alkaline phenotype. Nonetheless, expression of PhoU in *trans* did allow RmP3197 (Δ*phoU1*) to grow like the wildtype in MOPS-LPi, MOPS-HPi, MOPS-AEP and M9 media.

In order to further understand the role of PhoU in *S. meliloti*, we need to further study the *S. meliloti* Δ*phoU* strain RmP3197 and determine whether if it contains a suppressor mutation. Because based on the conjugation frequency of generating a *phoU* deletion using FLP-FRT recombination it seems that most of the colonies were not viable on LB media (Table 3). We were unable to complement the *phoU* deletion by expressing PhoU in *trans* in the Δ*phoU* isolated strain. Therefore we need to find a way to successfully complement the *phoU* deletion in RmP3197 (Δ*phoU1*); thereafter one can

mutate specific amino acid residues of PhoU and generate a functional map of PhoU. In order to determine the influence of PhoU on Pi transport by $PstSCAB_2$ transporter we need to generate a *S. meliloti* strain where the *pstSCAB* and *phoU* are expressed separately or together by an independent promoter such as *dme* (malic enzyme) in a Pi-transport negative (Δ*phoBΔpap-pit)* background. Then by performing a ^{33}Pi uptake assay we would be able to determine the influence of PhoU.

Figures

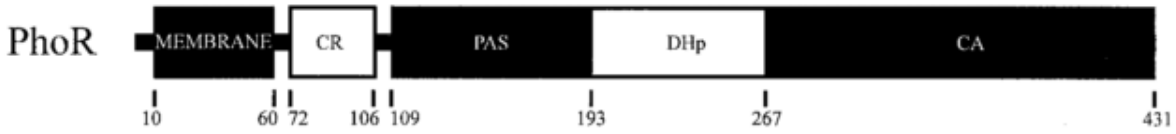

Figure 1: Domain structure of PhoR, taken from (23). The numbers on the bottom represent amino acid residues for *E. coli* PhoR. Membrane- transmembrane domain, CR- positively charged linker region, PAS- Per-Arnt-Sim domain, DHp- dimerization and histidine phosphoacceptor domain, CA- catalytic domain. No Periplasmic domain is present.

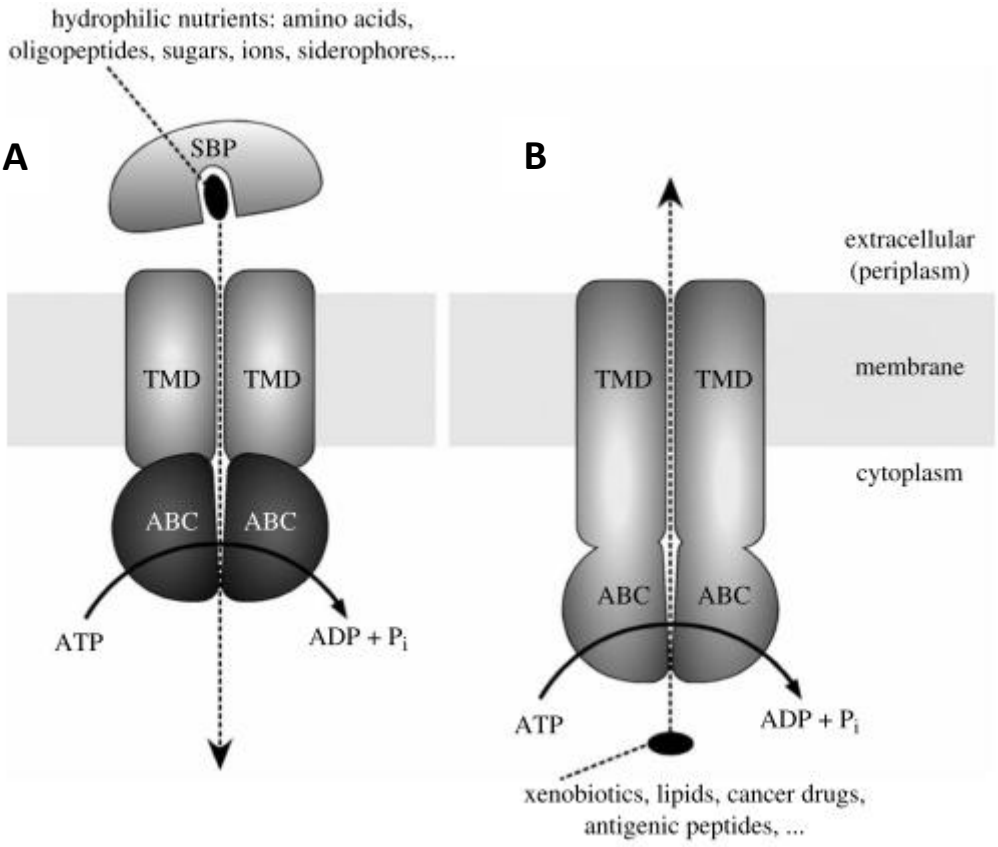

Figure 2: Schematic diagram of ABC transporter function, taken from (40). **A)** ABC importers, they require a substrate binding protein (SBP) which feeds the substrate into the translocation pathway formed by the TMDs. The ABCs (NBDs) are separate subunits. **B)** ABC exporters generally have their TMDs and ABCs (NBDs) fused together.

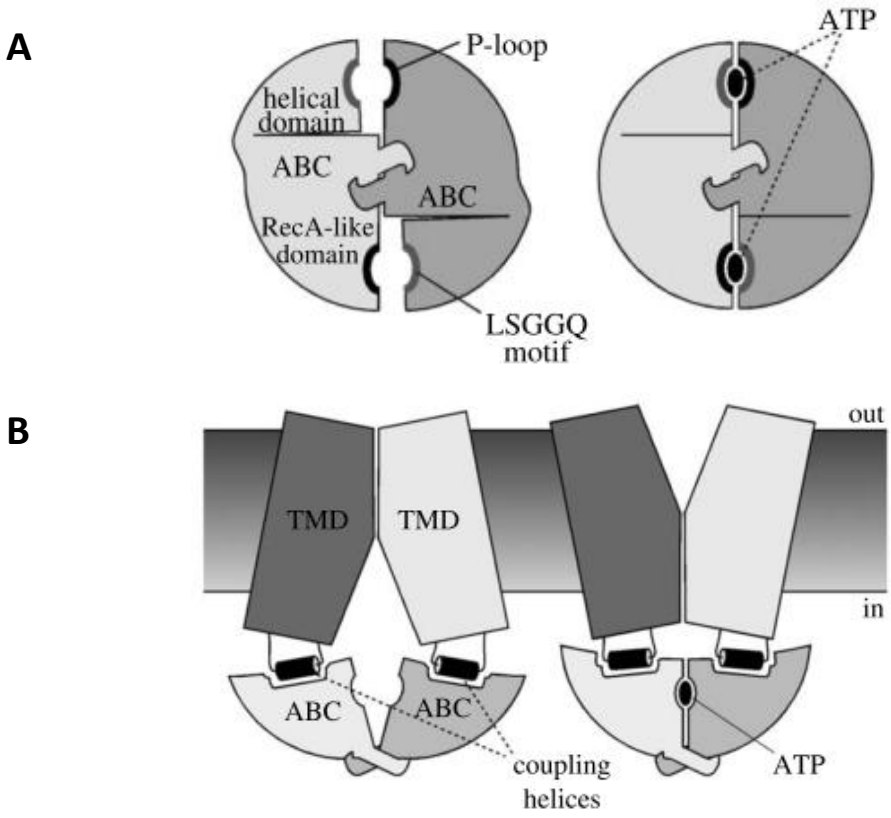

Figure 3: Coupling mechanism of ABC transporters, taken from (40). **A)** Binding sites for ATP in the NBDs. **B)** The molecular motion induced by binding of ATP triggers the closing of a gap between the ABCs. This moves the coupling helices closer together and flips the TMDs to an outward-facing conformation. Hydrolysis of ATP and subsequent release of the hydrolysis product reverts the TMDs to inward-facing conformation.

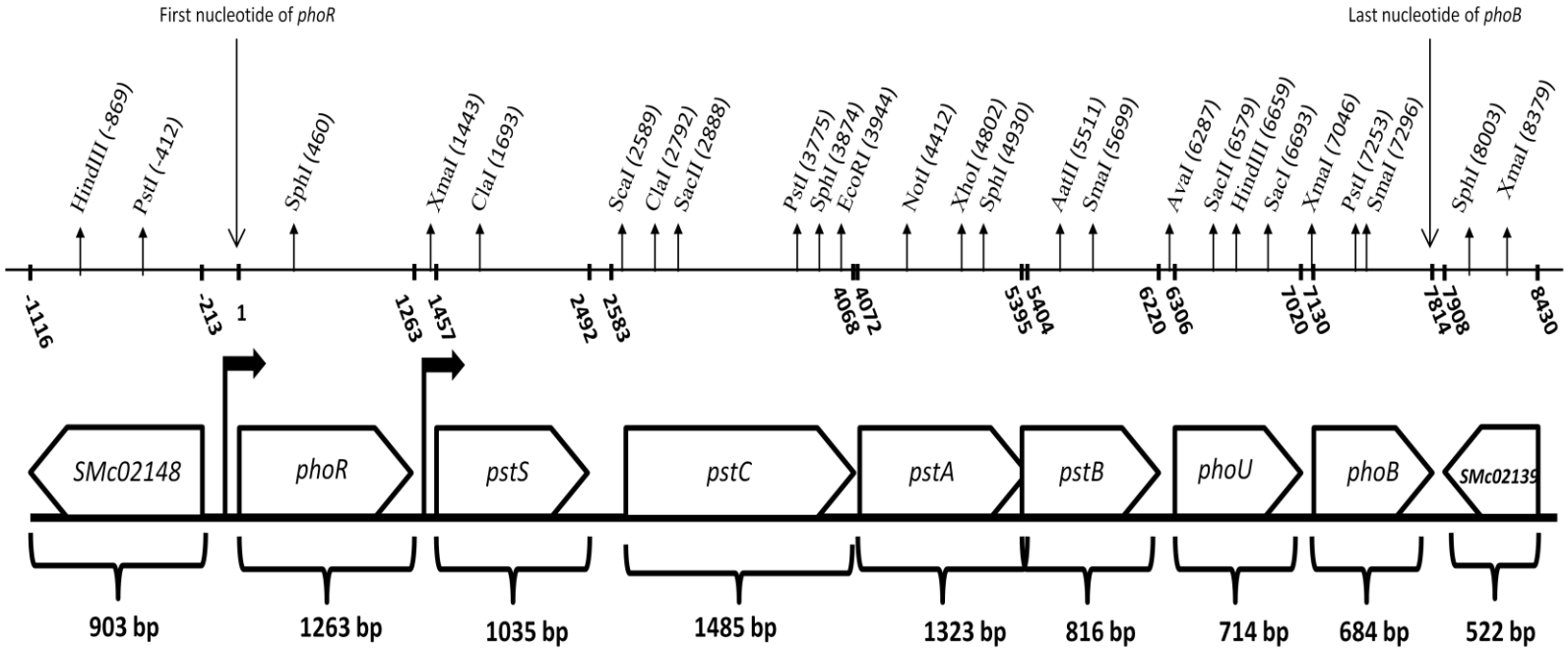

Figure 4: Diagram of the *pstSCAB* operon of *S. meliloti*, showing genes open reading frame (ORF) and unique restriction sites present within the operon

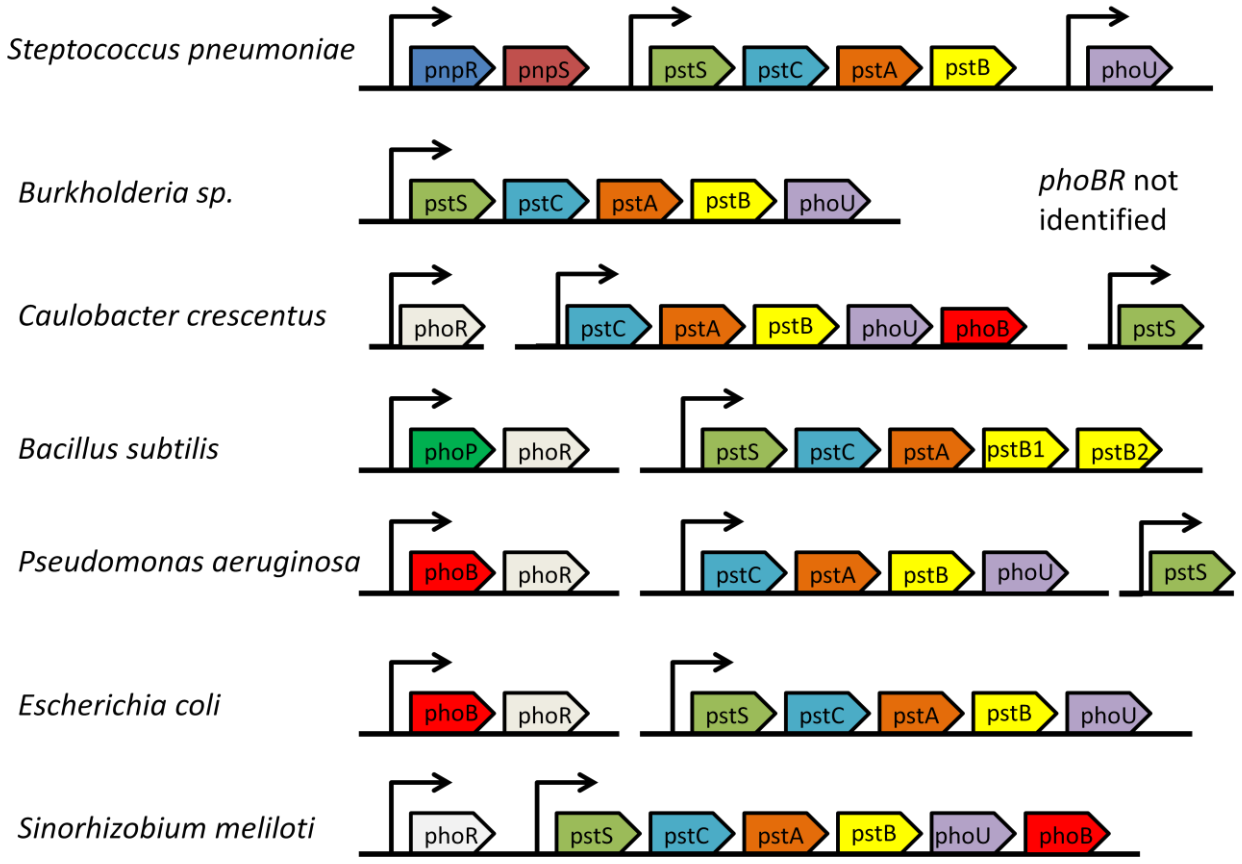

Figure 5: Comparison of the pst gene cluster in different bacteria. Arrow indicates the promoter and its direction. This figure is not to scale.

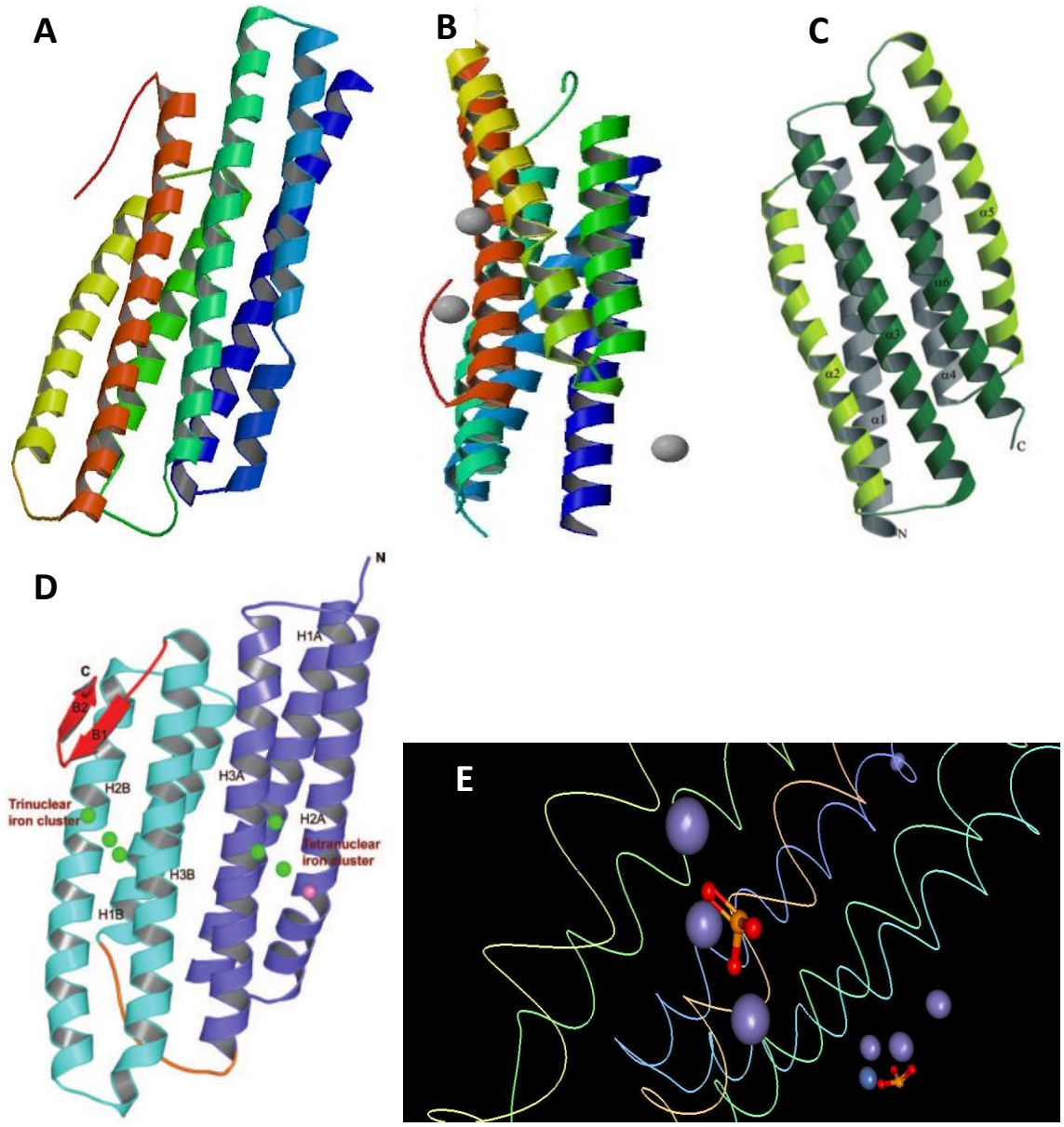

Figure 6: Ribbon diagram of PhoU crystal structures from **A)** *Geobacillus stearothermophilus* (PDB: 1XWM), **B)** *Streptococcus pneumonia* (PDB: 2I0M), **C)** *Aquifex aeolicus* (PDB: 1T72) taken from (64), **D)** *Thermotoga maritime* (PDB: 1SUM) taken from (65). The ribbon structure in **D)** of *T. maritime* does not show phosphite, thus figure **E)** shows binding of phosphite to the tetranuclear and trinuclear iron clusters separately. In **D)** iron and nickel ions are shown in green and pink circles respectively, whereas in **E)** iron and nickel ions are shown in purple and blue respectively and the phosphite molecule is shown in orange and red.

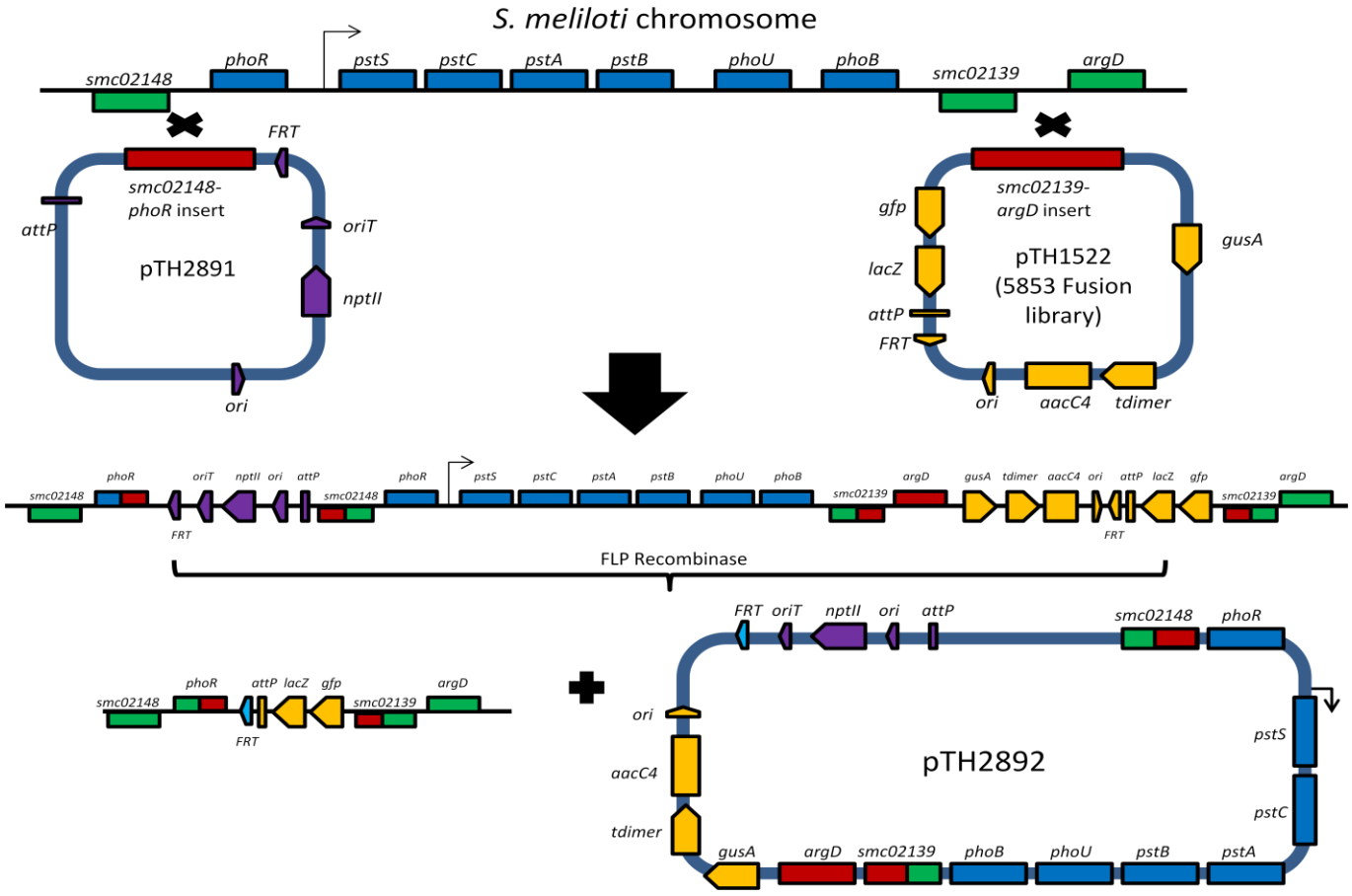

Figure 7: A schematic diagram of using FRT targeting vectors pTH1937 and pTH1522 to clone *S. meliloti phoR-pstSCAB-phoU-phoB* region of a plasmid. Plasmids pTH1522 and pTH1937 carrying homologous region of *S. meliloti* chromosome were recombined onto the chromosome. Thereafter using FLP-FRT recombinase system, the segment of DNA between two FRT sites was eliminated forming plasmid pTH2892 and captured using *E. coli* recipient strain. Diagram not to scale.

```
CLUSTAL 2.1 multiple sequence alignment


sp|P0A9K7|PHOU_ECOLI        MDSLNLNKHISGQFNAELESIRTQVMTMGGMVEQQLSDAITAMHNQDSDLAKRVIEGDKN 60
lcl|phoU                    ----MSHAHIMSAFDEELKYLTRRISEMGGLAEQMVADSVRALVNSDLALAQKVISDDTI 56
                                  : ** . *: **: :  ::  ***:.** ::*:: *: *.*  **::**..*.

sp|P0A9K7|PHOU_ECOLI        VNMMEVAIDEACVRIIAKRQPTASDLRLVMVISKTIAELERIGDVADKICRTALEKFSQQ 120
lcl|phoU                    LDDAERQIGEKAIVTIAKRQPMASDLREIMGSIRIAADLERVGDLGKNTAKRVIAVAGSG 116
                            ::  *  *.* .:  ****** ***** :*   :  *:***:**:..: .: .:   ..

sp|P0A9K7|PHOU_ECOLI        HQPLLVS-LESLGRHTIQMLHDVLDAFARMDIDEAVRIYREDKKVDQEYEGIVRQLMTYM 179
lcl|phoU                    IPRKLARGLEHLAELALVQLKEVLDVYASRSPEKANSIRERDEEIDAIYTSLFRELLTYM 176
                                *.  ** *.. ::  *::***.:*  . ::*  * ..*:::*  * .:.*:*:***

sp|P0A9K7|PHOU_ECOLI        MEDSRTIPSVLTALFCARSIERIGDRCQNICEFIFYYVKGQDFRHVGGDELDKLLAGKDS 239
lcl|phoU                    MEDPRNITPCTHLLFCAKNIERIGDHATNIAETIYYMATGAQPQGERPKDDMTSTLGSVT 236
                            ***.*.*..    ****:.******:. **.* *:* ..* : :    .:  .   *. :

sp|P0A9K7|PHOU_ECOLI        DK 241
lcl|phoU                    D- 237
```

Figure 8: Using ClustalW from EMBL-EBI, global sequence alignment between the *E. coli* PhoU protein sequence (sp|P0A9K7|PHOU_ECOLI) and *S. meliloti* PhoU protein sequence (lcl|phoU). There is 35% sequence identity and 66% sequence similarity between the two PhoU protein sequences.

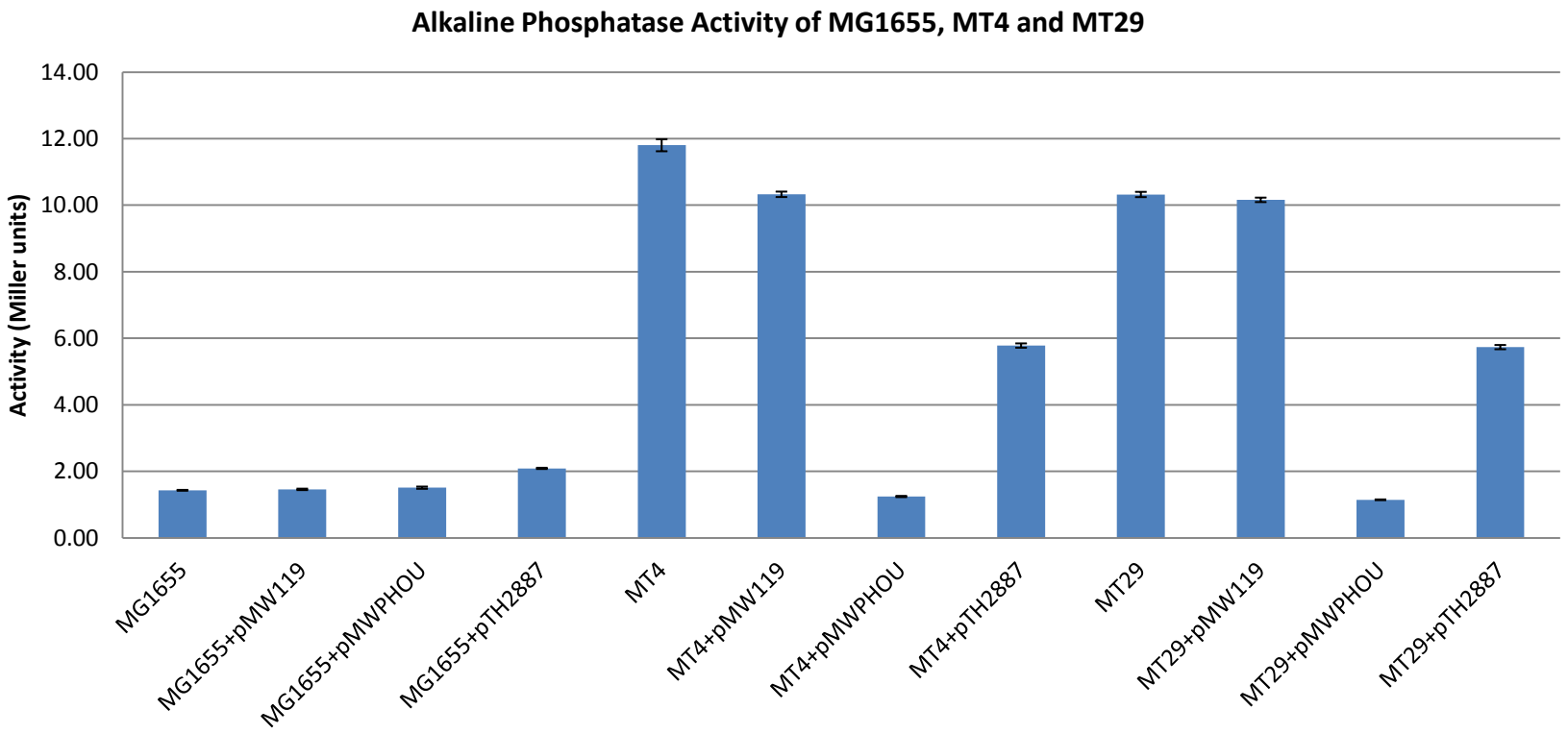

Figure 9: Quantitative alkaline phosphatase activities for *E. coli* MG1655 (wildtype), MT4 (*phoU* mutant) and MT29 (*phoU* mutant) with and without pMW119 (empty plasmid), pMWphoU (pMW119 with *E. coli phoU*) and pTH2887 (pMW119 with *S. meliloti phoU*) plasmids strains. All strains were grown in LB overnight, prior to assay and all experiments were done in triplicate.

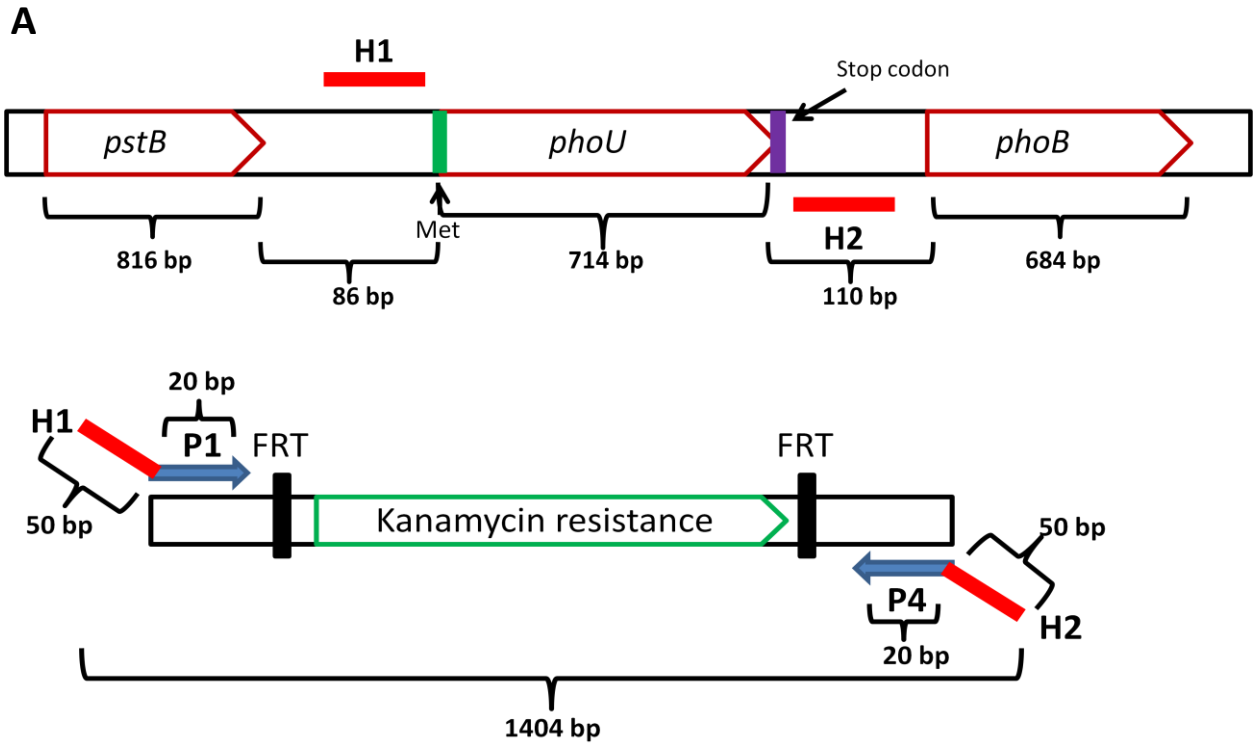
A
H1
Stop codon
pstB
phoU
phoB
Met
H2
816 bp
86 bp
714 bp
110 bp
684 bp
20 bp
H1
P1
FRT
FRT
50 bp
Kanamycin resistance
50 bp
P4
H2
20 bp
1404 bp

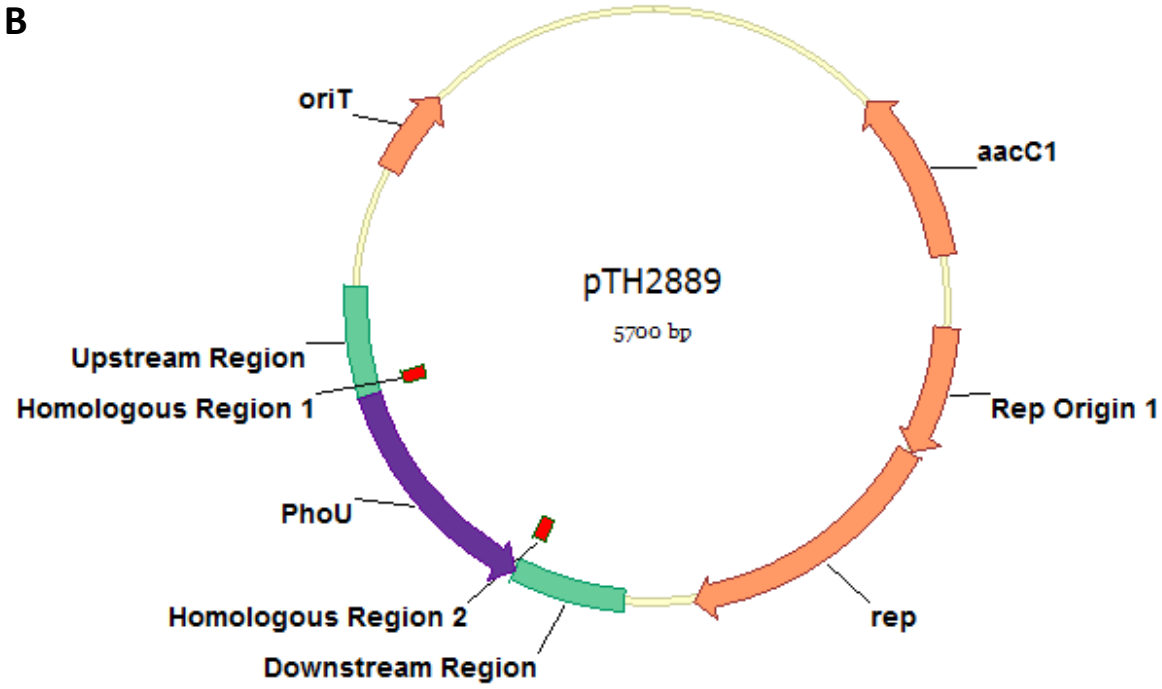
B
oriT
aacC1
pTH2889
5700 bp
Upstream Region
Homologous Region 1
Rep Origin 1
PhoU
Homologous Region 2
rep
Downstream Region

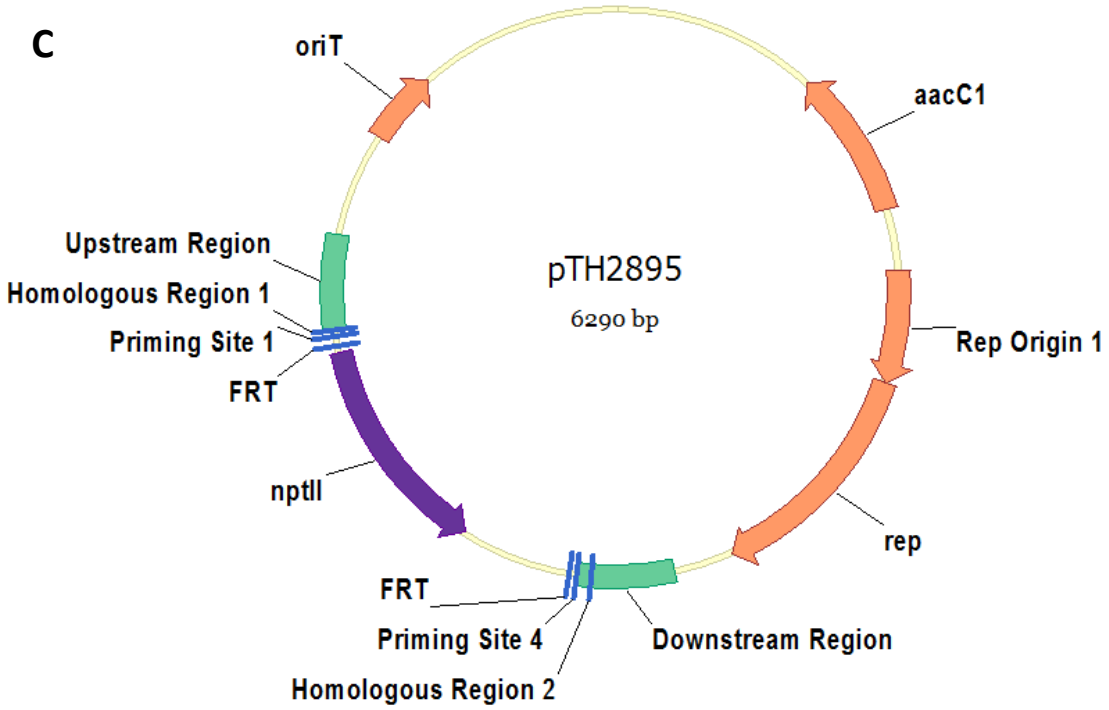

Figure 10: A schematic showing the three steps involved in replacing the *phoU* gene region with the Km/Nm cassette flanked by FRT sites. **A)** The Km/Nm cassette was PCR amplified from pKD13 using the primers PKD13-KanF1 and PKD13-KanR1. In red squares, the two 50-nt homologous ends attached to the PCR primers are shown relative to their location on the chromosome. **B)** Plasmid pTH2889 contains the *S. meliloti phoU* flanked by the *S. meliloti* 340bp upstream and 352bp downstream regions in the pUCP30T plasmid. **C)** Plasmid pTH2895 was derived from pTH2889 and the *phoU* gene is replaced by the Km/Nm cassette flanked by FRT sites. The region between *nptII* gene and priming site 4 is part of the PCR product insertion amplified from pKD13 plasmid. Figure not to scale.

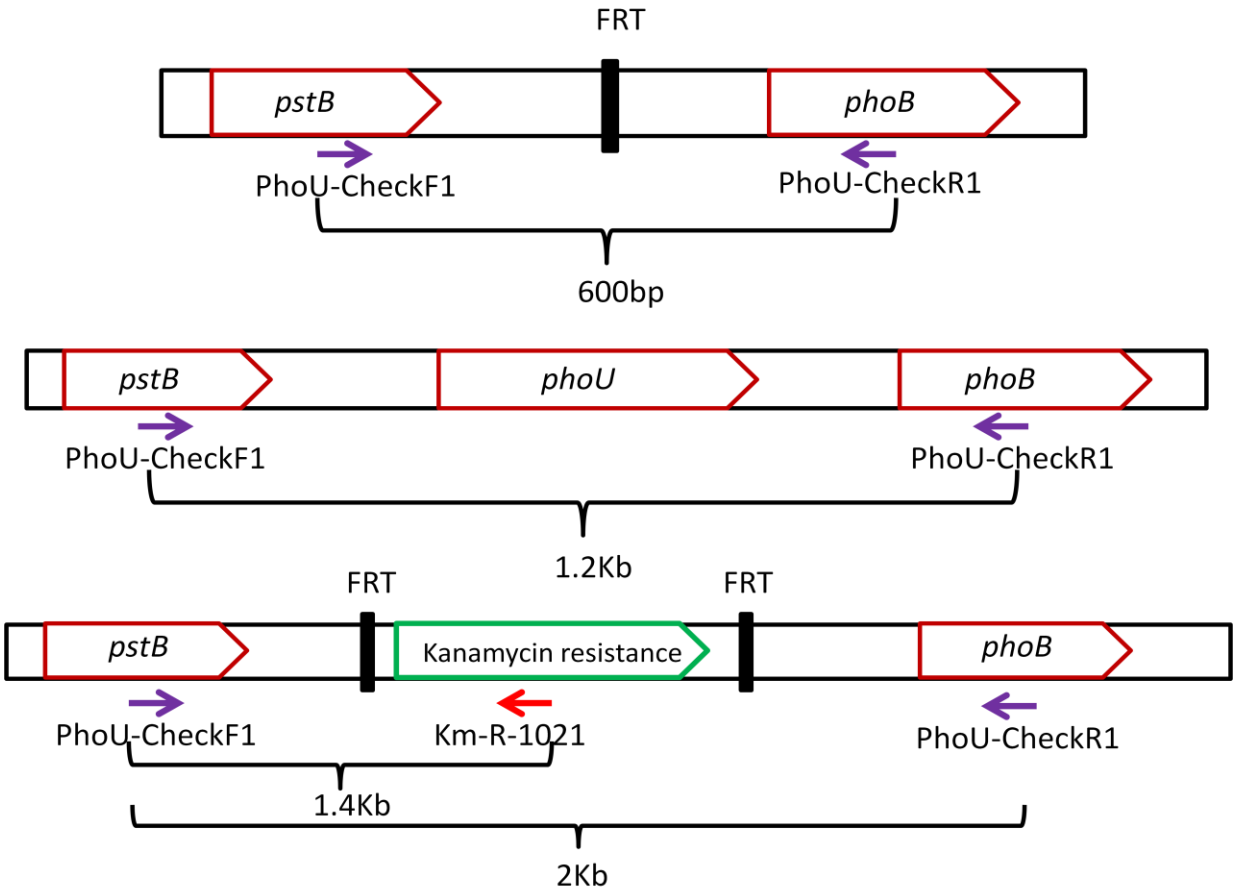

Figure 11: Diagram showing the binding sites for PCR primers and the size of the PCR fragments expected in verifying the loss of the Kanamycin resistance cassette from the chromosome of the Δ*phoU*::Km strain. PhoU-CheckF1 and PhoU-CheckR1 bind to upstream (*pstB)* and downstream (*phoB*) of *phoU*. The Km-R-1021 primer specifically binds to the Km-cassette insertion. PhoU-CheckF1 and PhoU-CheckR1 primers (Primer set 1) should generate a 600bp size fragment in the *S. meliloti* Δ*phoU* strain and a 1.2Kb size fragment from wildtype RmP110 DNA. They should generate a 2Kb fragment if the Km-cassette is present. The PhoU-CheckF1 and Km-R-1021 primers (Primer set 2) should generate a 1.4 Kb fragment when the Km-cassette insertion is present. This figure is not to scale.

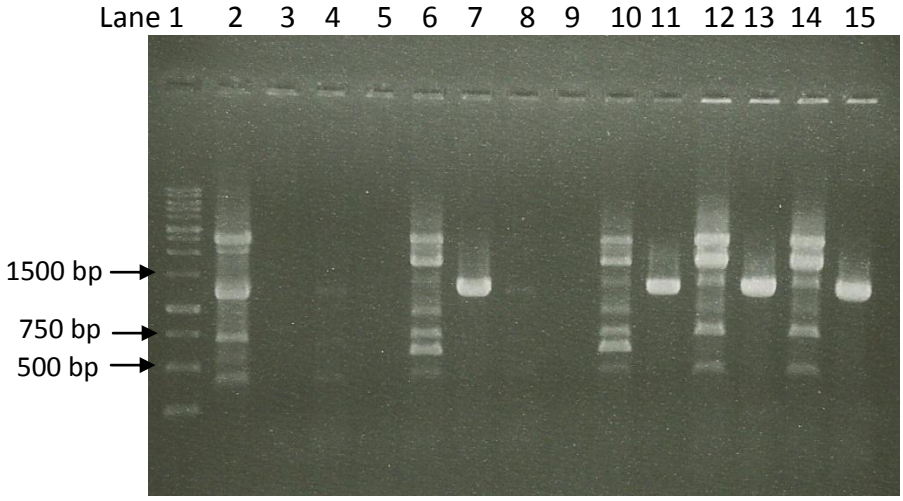

Primer set 1: PhoU-CheckF1 and PhoU-CheckR1
Primer set 2: PhoU-CheckF1 and Km-R-1021

Lane: Sample

1: 1Kb DNA ladder RTU (FroggaBio)
2: *S. meliloti* RmP110 - Primer set 1
3: *S. meliloti* RmP110 - Primer set 2
4: Background colony 1 - Primer set 1
5: Background colony 1- Primer set 2
6: Transconjugant 1 – primer set 1
7: Transconjugant 1 – primer set 2
8: Background colony 2 - Primer set 1
9: Background colony 2 - Primer set 2
10: Transconjugant 2 – primer set 1
11: Transconjugant 2 – primer set 2
12: RmP3198 (*ΔphoU2*::Km) – Primer set 1
13: RmP3198 (*ΔphoU2*::Km) – Primer set 2
14: *S. meliloti* with Km-cassette insertion 2 – Primer set 1
15: *S. meliloti* with Km-cassette insertion 2 – Primer set 2

Figure 12: Analysis of pTH2505 Flp-plasmid transconjugants obtained on LB media following transfer of pTH2505 into RmP3198 (Δ*phoU2*::Km/Nm). Colonies were examined by whole cell PCR. PCR product was run on an agarose gel, designed to determine whether Km-cassette insertion has been eliminated from the chromosome after FLP-recombinase conjugation with. For the location of primer pairs, see Fig. 10. Primer set 1 generate a 1.2Kb fragment in wildtype RmP110 and a 600bp size fragment in *phoU* deletion strains. Primer set 2 should only amplify a fragment if the Km-cassette is present on the chromosome. The presence of 600bp and 1.4kb size fragment in lane 6/7 and 10/ 11 suggests that some cells have the Km-cassette eliminated while other still have Km-cassette on their chromosome. Three molecular weight markers have been labeled and 'bp' refers to 'base pairs'. The PCR had an annealing temperature of 58^{o}C and an elongation time of 110 seconds.

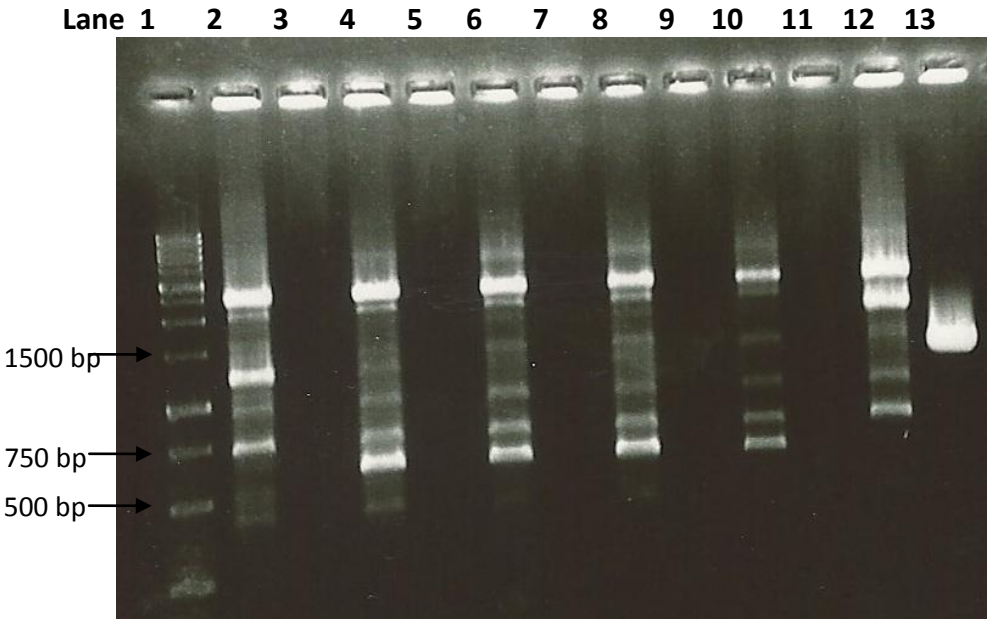

Primer set 1: PhoU-CheckF1 and PhoU-CheckR1
Primer set 2: PhoU-CheckF1 and Km-R-1021

Lane: Sample

1: 1Kb DNA ladder RTU (FroggaBio)
2: *S. meliloti* RmP110 - Primer set 1
3: *S. meliloti* RmP110 - Primer set 2
4: RmP3197 (*S. meliloti ΔphoU1*) - Primer set 1
5: RmP3197 (*S. meliloti ΔphoU1*) - Primer set 2
6: Transconjugant 2 (*S. meliloti ΔphoU*) – primer set 1
7: Transconjugant 2 (*S. meliloti ΔphoU*) – primer set 2
8: Transconjugant 3 (*S. meliloti ΔphoU*) - Primer set 1
9: Transconjugant 3 (*S. meliloti ΔphoU*) - Primer set 2
10: Transconjugant 4 (*S. meliloti ΔphoU*) – primer set 1
11: Transconjugant 4 (*S. meliloti ΔphoU*) – primer set 2
12: RmP3198 (*ΔphoU2*::Km) – Primer set 1
13: RmP3198 (*ΔphoU2*::Km) – Primer set 2

Figure 13: Analysis of pTH2505 Flp-plasmid transconjugants obtained on MOPS- AEP media following transfer of pTH2505 into RmP3198 (Δ*phoU2*::Km/Nm). Result of a whole cell PCR, run on an agarose gel, designed to determine whether Km-cassette insertion has been eliminated from the chromosome after FLP-recombinase conjugation with RmP3198. Primer set 1 should generate a 1.2Kb fragment in wildtype RmP110 and a 600bp size fragment in *phoU* deletion strains. Primer set 2 should only amplify a fragment if the Km-cassette is present on the chromosome. The presence of 600bp fragment in lanes 4, 6, 8 & 10 and lack of 1.4Kb fragment in lanes 5, 7, 9 & 11 confirm that all transconjugant (including RmP3197 (*ΔphoU1*)) cells have the Km-cassette eliminated from their chromosome. Selected molecular weight markers have been labeled and 'bp' refers to 'base pairs'. The PCR had an annealing temperature of 58^{o}C and an elongation time of 110 seconds.

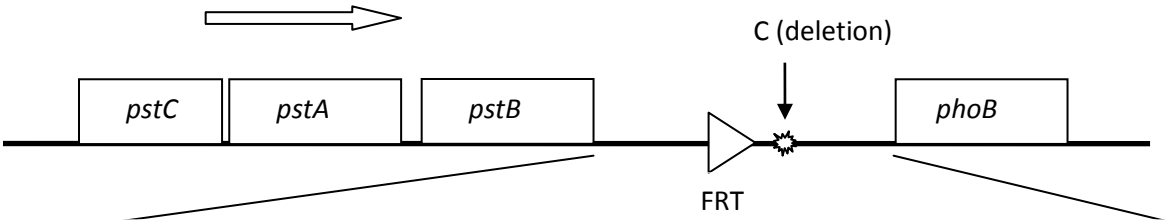

TGATGGCGAGAGGGGCGGCGCTTTTCCGTCCCTCCCGGTTTAAGATCGACCGAGCCATTCAGAACAGCGCGTCTC
CCGAGGAAACGAATGTGTAGGCTGGAGCTGCTTC**GAAGTTCCTATACTTTCTAGAGAATAGGAACTTCG**AACTGC
AGGTCGACGGATCCCCGGAATGATCGCCCGGCATCCGGGCCTATGCAGAATTTGTTCCGGCCGCTTTGGCGCGGC
CTACCACCGTGCGCGGCGGCATGACGGCTGTCGTGCGTAGGAAGGAGTCCTACTGAATG

Figure 14: Diagram showing the sequence from the PCR product of intergenic sequence between *pstB* and *phoB* of *S. meliloti* strain RmP3197 (*ΔphoU1*). 82-bp scar region generated after FLP-FRT recombination is highlighted in green with FRT site underlined. Stop codon (TGA) of *pstB* is highlighted in red and start codon (ATG) of *phoB* is shown in blue. Also the location of the 1-nt deletion in the intergenic region between FRT site scar and *phoB* is also highlighted (Red "C"). Open arrow indicates direction of transcription.

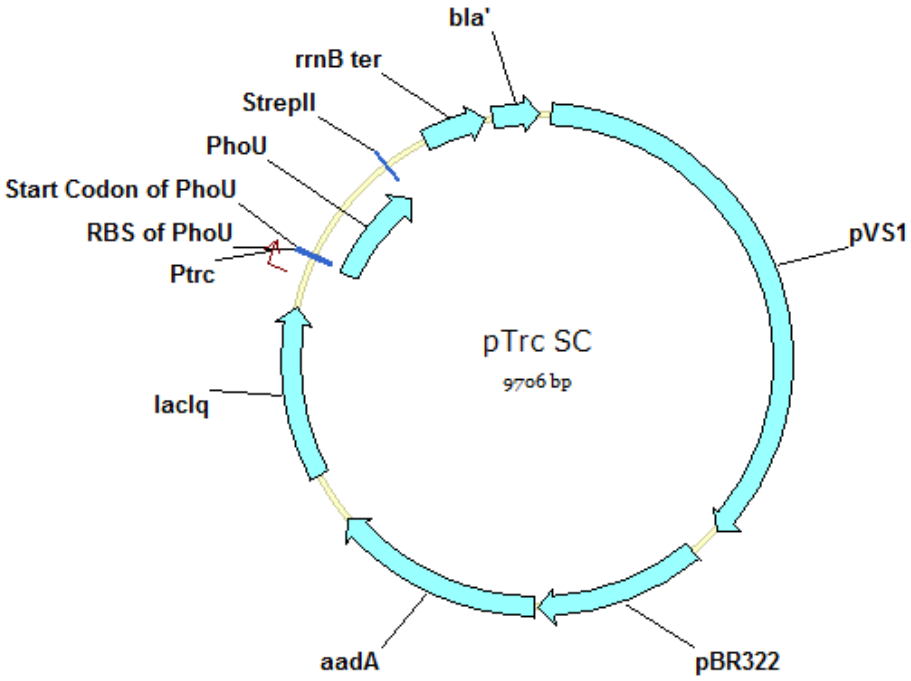

Figure 15: Plasmid map of pTH2888, *S. meliloti phoU* in pTrc plasmid.

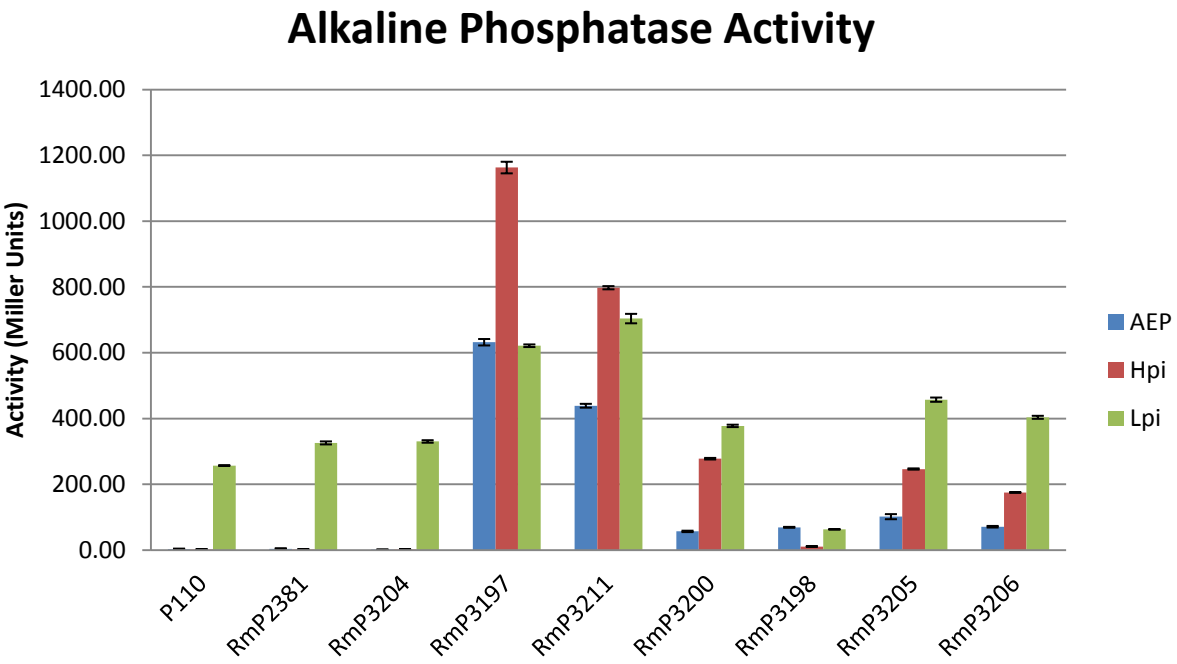

Figure 16: Alkaline phosphatase activity of *ΔphoU* strains in MOPS LPi, HPi and AEP media. Refer to table 1 for strain genotypes. The wildtype P110 strain show alkaline phosphatase activity in only low phosphate media as expected. The non-polar *phoU* mutants strains (RmP3197 and RmP3211) express alkaline phosphatase activity in all condition tested. The polar *phoU* mutant (RmP3198, Δ*phoU2*::Km) has low alkaline phosphatase activity in all conditions. The *phoU* mutant strains with *S. meliloti* PhoU expressed in *trans* (RmP3200, RmP3205 and RmP3206) partially complement the alkaline phosphatase activity. All samples were in triplicate. Error bars represent standard error between samples.

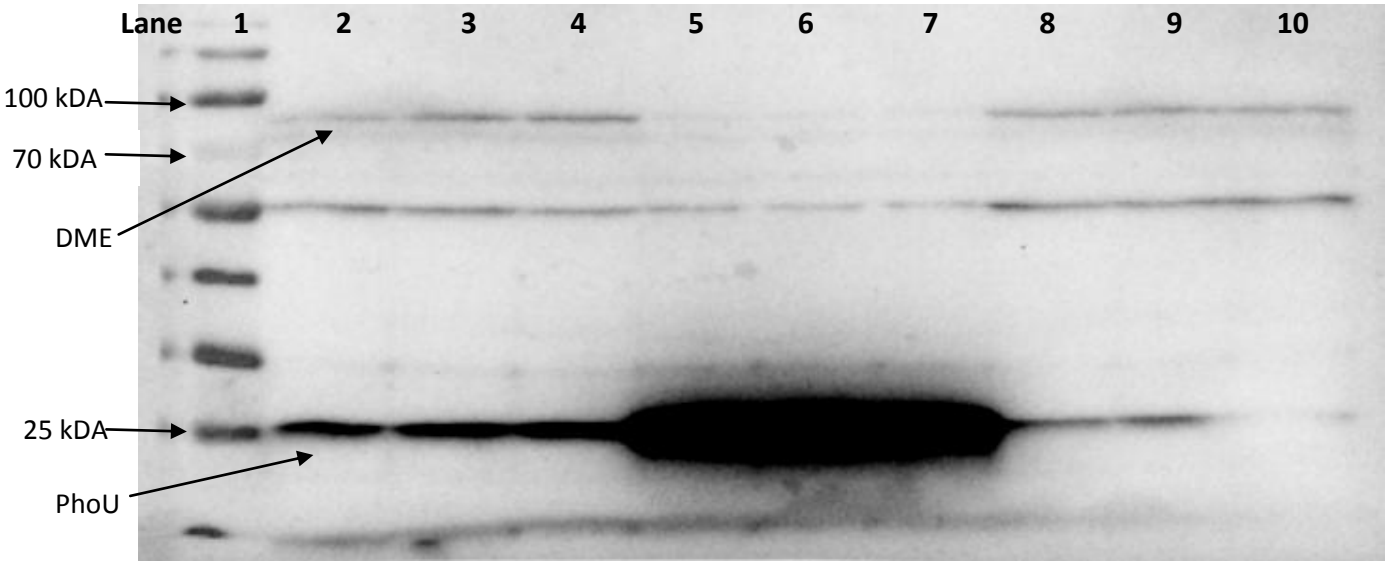

Figure 17: Western blot of *S. meliloti* RmP110 strain (wildtype) grown in MOPS-AEP, MOPS-LPi and MOPS-HPi media probed with anti-PhoU and anti-DME antibody. Lane 1 protein molecular weight standards of 10-170 kDa (25 kDA, 70 kDA and 100 kDa are labeled), Lane 2-4 RmP110 strain grown in MOPS-AEP, Lane 5-7 RmP110 strain grown in MOPS-LPi and Lane 8-10 RmP110 strain grown in MOPS-HPi. PhoU is present in all samples at molecular weight of 27kDa and DME is present at ~87kDa. PhoU is highly expressed in LPi media compared to the AEP or HPi media. This western blot was used for chemiluminescence and the amount of PhoU protein was quantified and the DME protein was used as a housekeeping protein to standardize all samples.

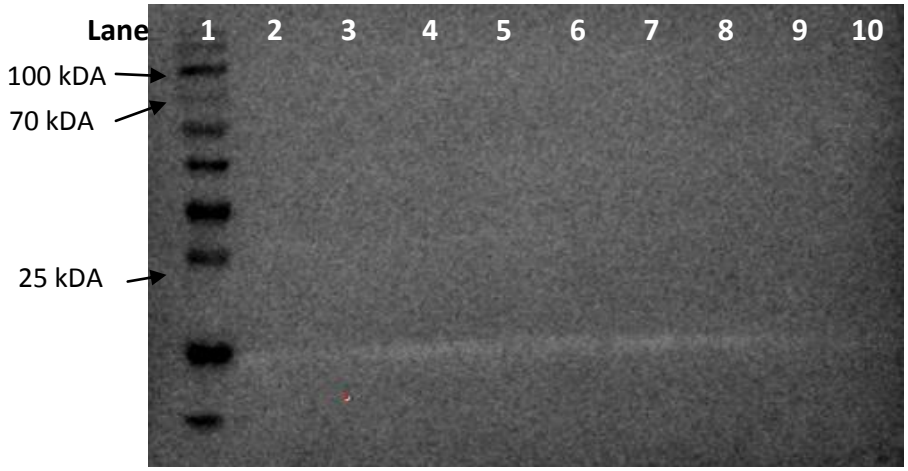

Figure 18: Western blot of RmP3211 (*ΔphoU1* with pTrc) strain grown in MOPS-AEP, MOPS-LPi and MOPS-HPi media probed with anti-PhoU and anti-DME antibody. Lane 1 protein molecular weight standards of 10-170 kDa (25 kDA, 70 kDA and 100 kDa are labeled), Lane 2-4 RmP3211 *S. meliloti ΔphoU* strain carrying pTH1931 (empty pTrc) plasmid grown in MOPS-AEP, Lane 5-7 RmP3211 strain grown in MOPS-LPi and Lane 8-10 RmP3211 strain grown in MOPS-HPi. No PhoU protein was detected in *phoU* mutant strain transformed with empty pTrc plasmid (pTH1944) in all media conditions. A similar result was seen with RmP3197 strain (data not shown).

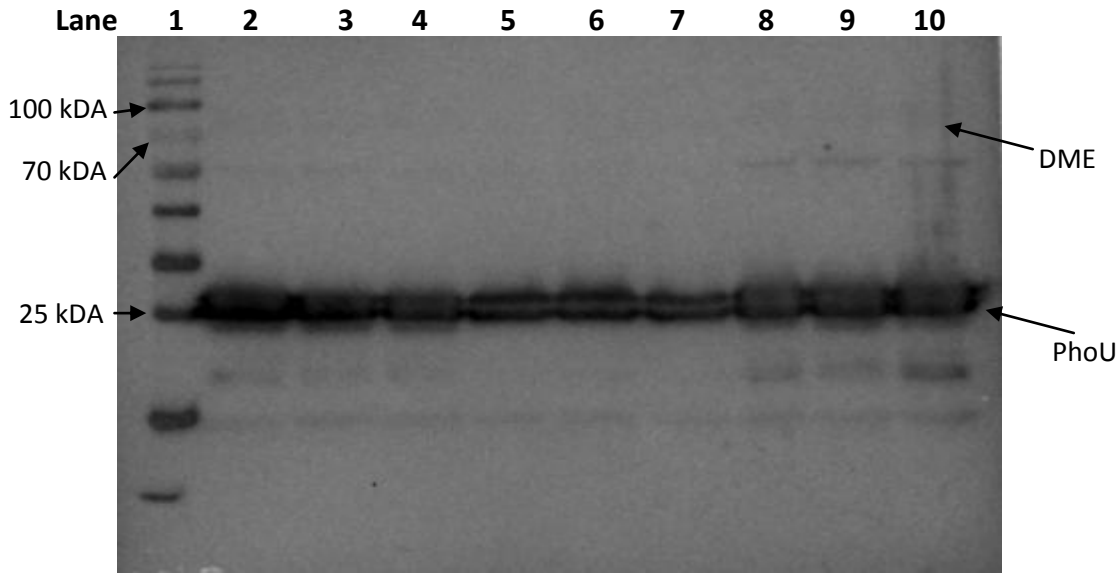

Figure 19: Western blot of RmP3204 (RmP110 with pTH2888) strain grown in MOPS-AEP, MOPS-LPi and MOPS-HPi media probed with anti-PhoU and anti-DME antibody. Expression of PhoU from pTH2888 (pTrc with *S. meliloti phoU*) we can observe that there are two bands present around ~27kDa. Also the amount of PhoU present in each of the three media conditions (Lane 1 protein molecular weight standards of 10-170 kDa, lanes 2-4 is MOPS- AEP, Lanes 5-7 is MOPS- LPi and Lanes 8-10 is MOPS- HPi) is approximately the same. The DME signal for these samples was faint and not clearly detected.

A **Growth curve of *phoU* mutant strains in MOPS-LPi (0.02mM Pi)**

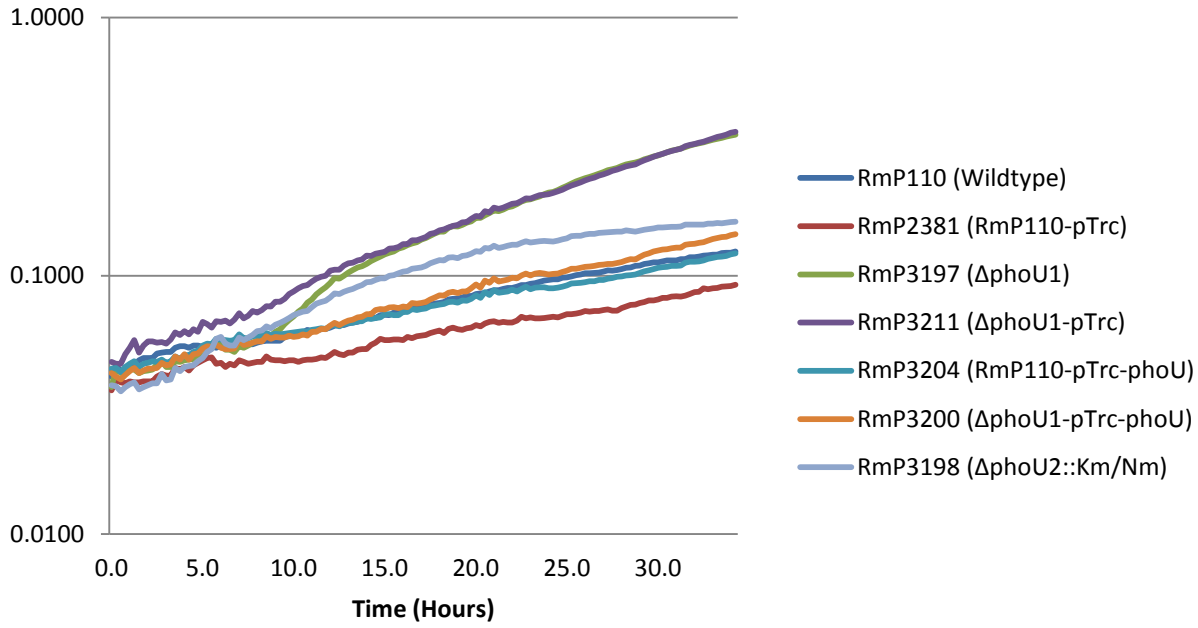

B **Growth curve of *phoU* mutant strains in MOPS-HPi (2mM Pi)**

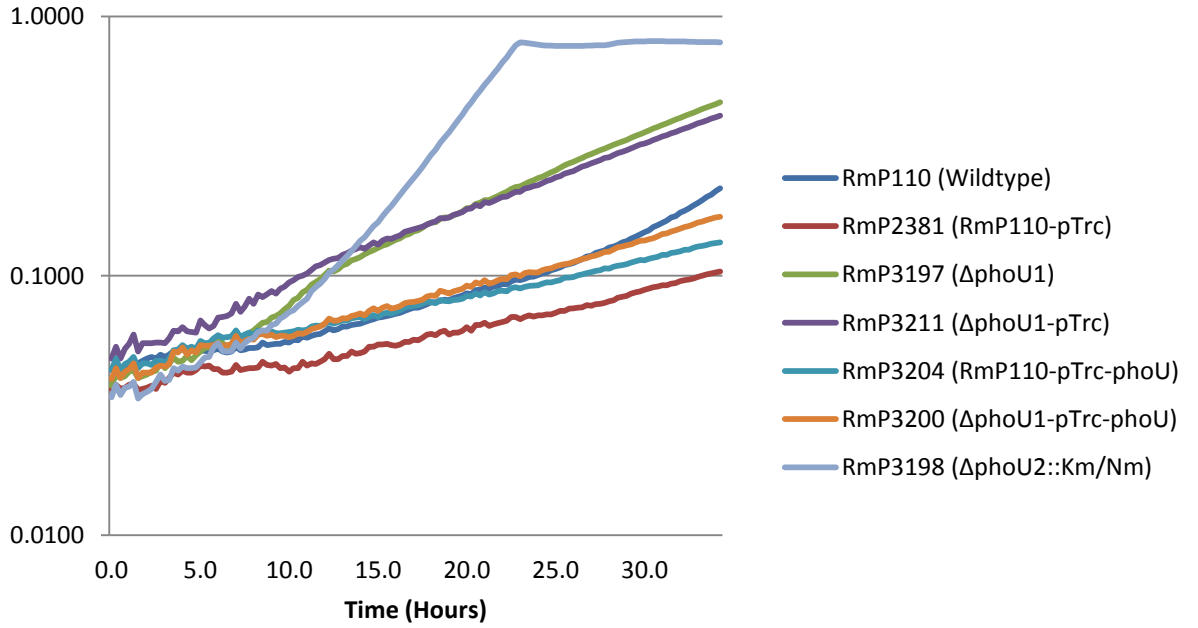

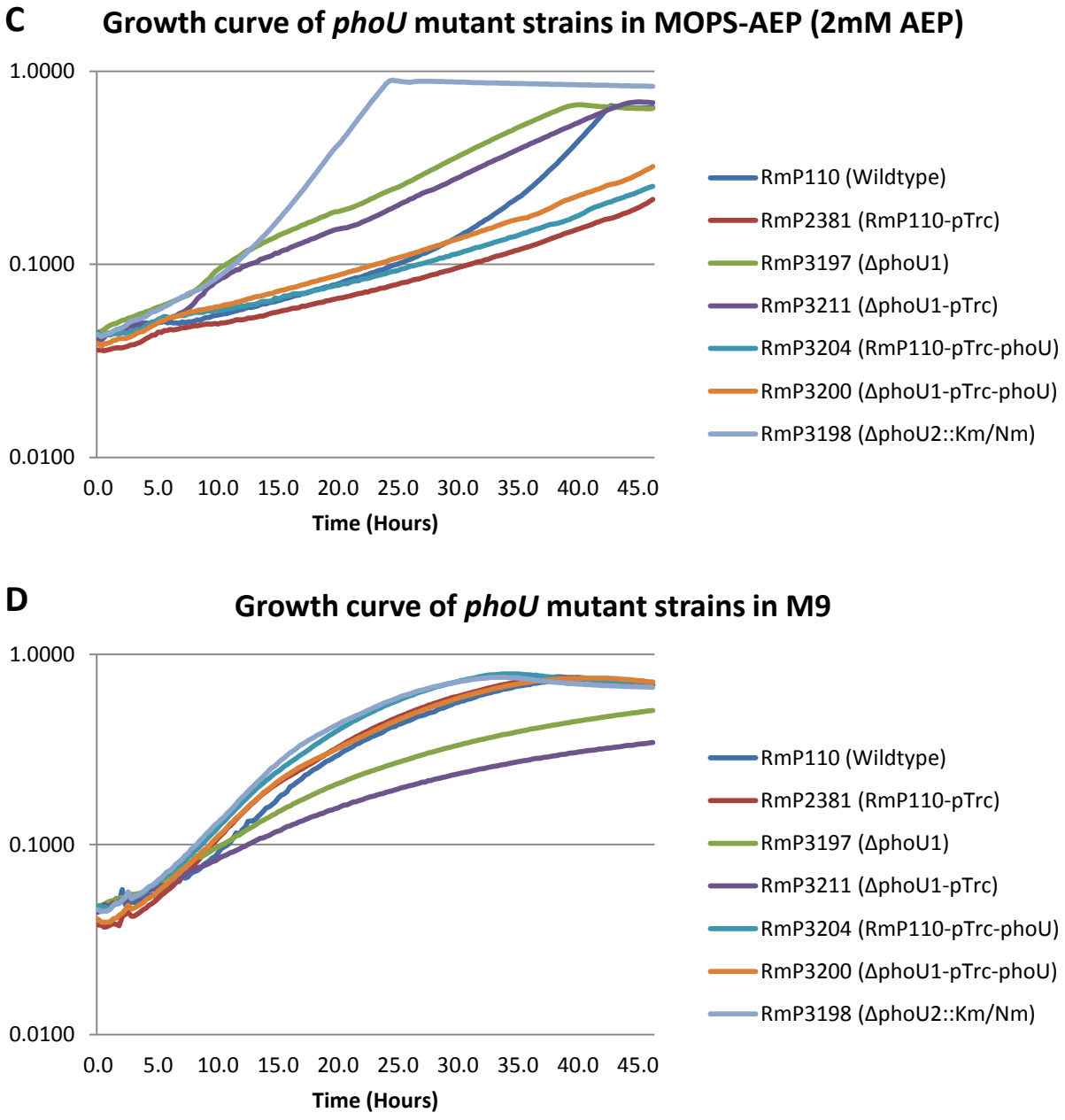

Figure 20: Growth curve of Δ*phoU* mutants containing the complementing plasmid in **A)** MOPS-LPi, **B)** MOPS-HPi, **C)** MOPS-AEP and **D)** M9 liquid media. Strains were grown at 30^{o}C. Refer to table 1 for genotype. Wildtype RmP110 was used as the positive control and blank media was used as negative control. Log_{10} values of measured OD_{600} reading are plotted. The growth curve machine stopped working after 34 hours for MOPS-LPi and MOPS-HPi, whereas MOPS-AEP and M9 media growth curve was ran for 46 hours. Data were collected every 15 minutes and each data point is average from three cultures.

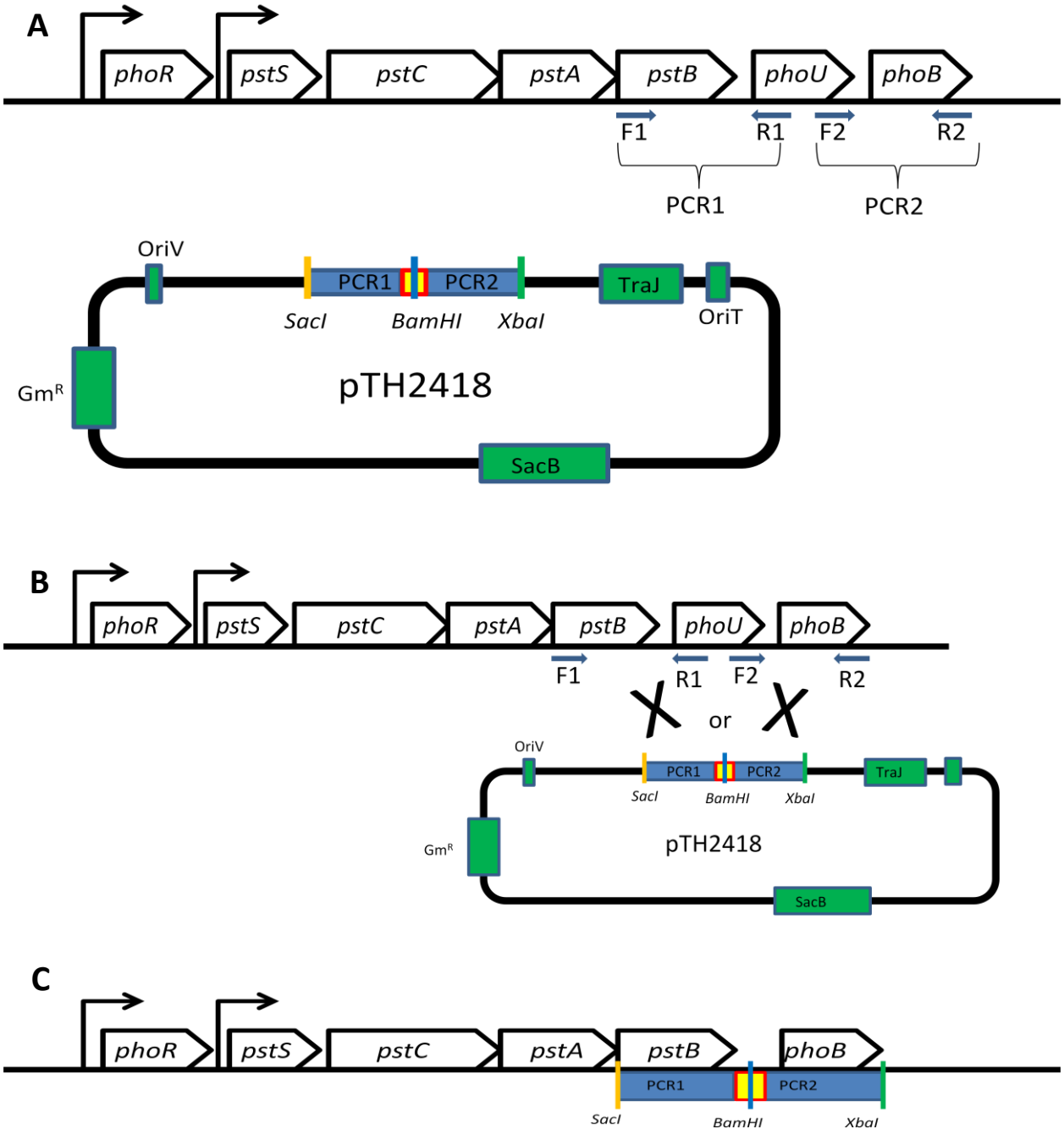

Figure 21: Steps of using *SacB* selection to generate unmarked *ΔphoU* strain **A)** Insertion of PCR1 + PCR2 (nt: 570657-571588 + nt: 572240-573078) in pJQ200mp18 plasmid between restriction sites *SacI, BamHI* and *XbaI*, generating plasmid pTH2418. **B)** A diagram highlighting recombination site between pTH2418 and *S. meliloti* chromosome. **C)** Diagram of unmarked *phoU* deletion on *S. meliloti* chromosome. This figure is not to scale.

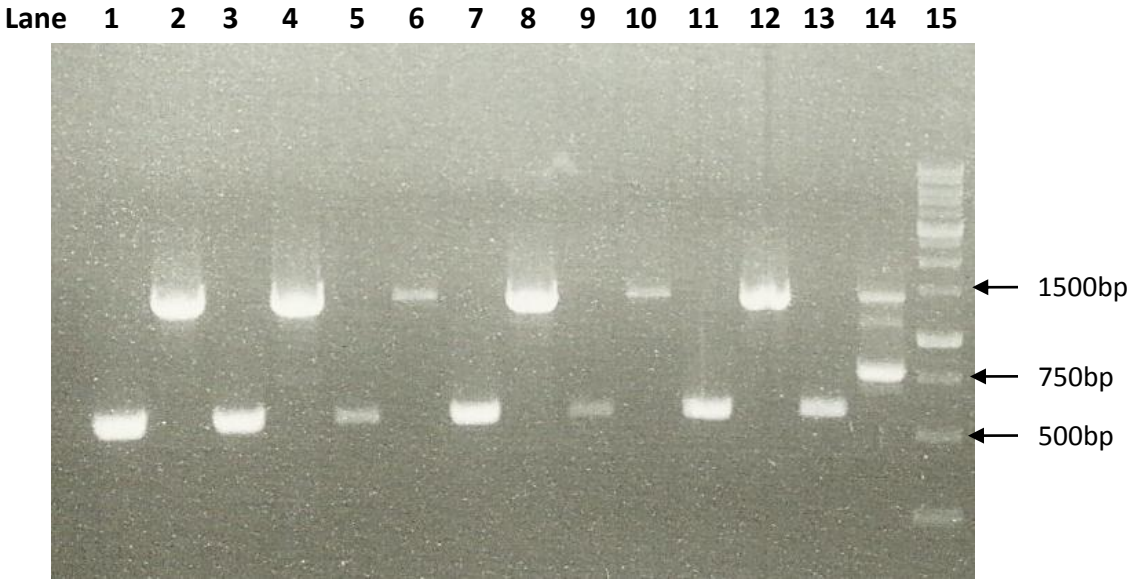

Lane: **Sample**
1: RmP110 – Primer set 1
2: RmP110 – Primer set 2
3, 5, 7, 9, 11 and 13: Primer set 1
4, 6, 8, 10, 12 and 14: Primer set 2
15: 1 kilobase molecular weight marker

Primer set 1: Pst-1937F and Pst-1937R
Primer set 2: DelphoUF and DelphoUR

Figure 22: Result of a whole cell PCR, run on an agarose gel, designed to determine whether an unmarked *phoU* deletion has been made. Primer set 1 should amplify a 600 bp chromosomal sequence upstream of the *phoR* and was used as a positive control in both wildtype RmP110 and transconjugants colonies. Primer set 2 should only amplify a fragment of 750bp if unmarked *phoU* deletion has been made, however if the deletion has not been made then a 1400bp PCR product will be generated. The presence of 600bp positive control gene is amplified in all transconjugants and in RmP110, lanes 1, 3, 5, 7, 9, 11, 13. As for primer set 2 PCR products, RmP110 and all transconjugants had 1400bp product lane 2, 4, 6, 8, 10, 12. However one of the transconjugant also had 750bp product along with 1400bp product. Three molecular weight markers are labeled. Based on the result no unmarked *phoU* deletion strain was obtained. 'bp' refers to 'base pairs'.

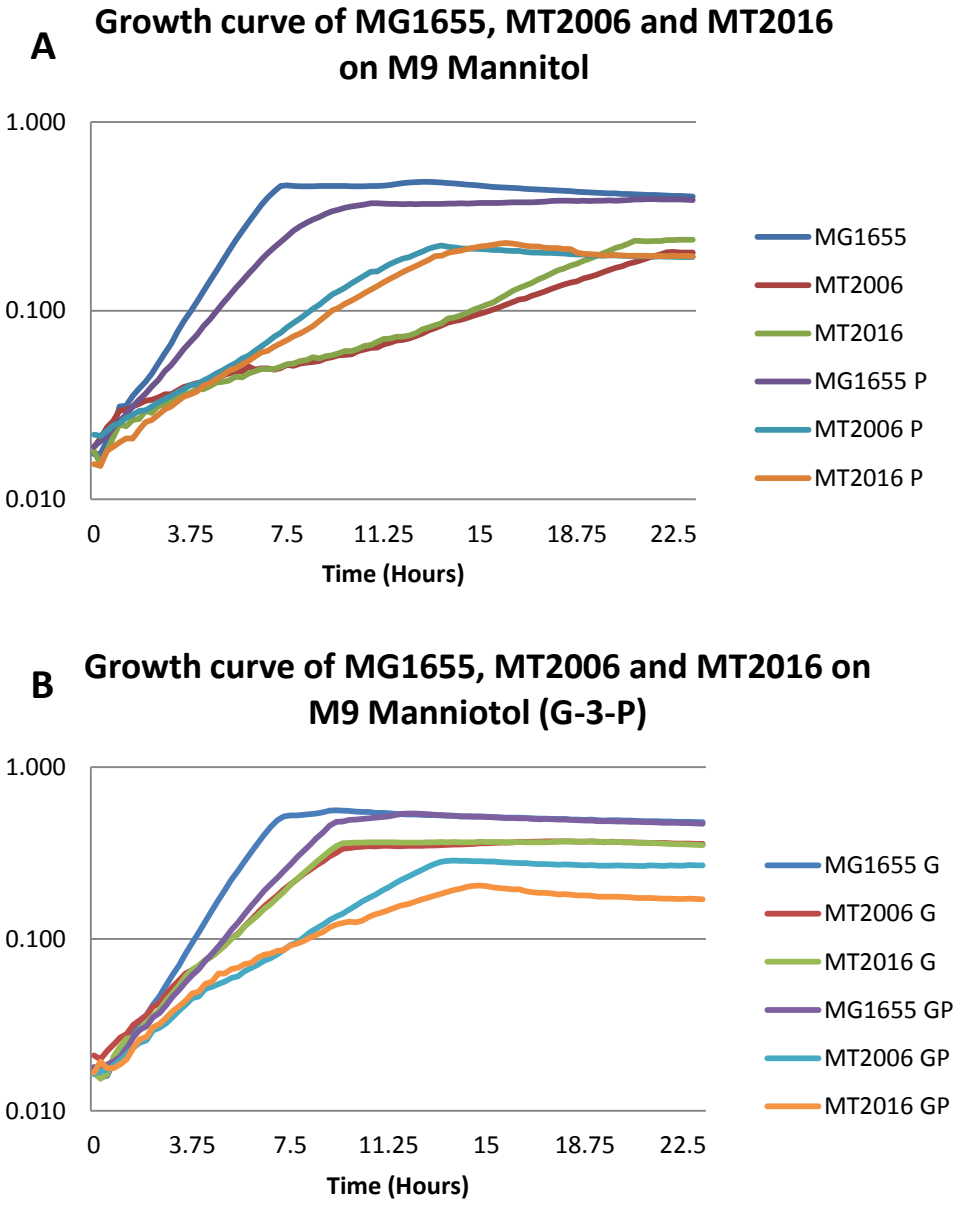

Figure 23: Growth curve of MG1655, MT2006 and MT2016 strains on **A)** M9 Mannitol media and **B)** M9 mannitol + G-3-P. Strains were grown for 24 hours at 37^{o}C. In legend: **P** symbolizes presence of plasmid pTH2892. **G** stands for G-3-P. **GP** stands for G-3-P and plasmid pTH2892. *S. meliloti* PstSCAB$_2$ transporter expressed from plasmid pTH2892 allowed MT2006 and MT2016 strains to grow on M9 mannitol media but not to the level of wildtype MG1655 strain.

Tables

Table 1: Bacterial strains, Plasmids and Primers

Strains and plasmids	Relevant characteristics	Source, reference, construction
Sinorhizobium meliloti		
RmP110	Rm1021 with changed wild-type *pstC*; Sm^R	Yuan *et al*. (2006)
RmP2381	*S. meliloti* RmP110 with pTH1931 (pTrc plasmid); Sm^R, $Spec^R$	Lab Collection
RmP3197	*S. meliloti* RmP110 ΔPhoU1; Sm^R	This study
RmP3198	*S. meliloti* RmP110 ΔPhoU2::Kanamycin cassette; Sm^R, Nm^R	This study
RmP3199	*S. meliloti* RmP110 ΔPhoU1- pTH628; Sm^R, Gm^R	This study
RmP3200	*S. meliloti* RmP110 ΔPhoU1- pTH2888 (PtrcPhoU); Sm^R, $Spec^R$	This study
RmP3201	*S. meliloti* RmP110 (pTH628); Sm^R, Gm^R	This study
RmP3202	Rmfl 5853 + pTH2891 (pTH1937 with insert sMC02148) (Recombined into chromosome); Gm^R, Nm^R	This study
RmP3203	*S. meliloti* RmP110 Truncated ΔPhoU3:: Kanamycin cassette; Sm^R, Nm^R	This study
RmP3204	*S. meliloti* RmP110 with pTH2888 (ptrc-phoU); Sm^R, $Spec^R$	This study
RmP3205	*S. meliloti* RmP110 ΔPhoU4 with pTH2888 (ptrcphoU) (deletion made in trans); Sm^R, $Spec^R$	This study
RmP3206	*S. meliloti* RmP110 Truncated ΔPhoU5 with pTH2888 (ptrcphoU) (deletion made in trans); Sm^R, $Spec^R$	This study
RmP3207	*S. meliloti* RmP110 ΔPhoU2::Kanamycin cassette with pTH1931(ptrc); Sm^R, Nm^R	This study
RmP3208	*S. meliloti* P110 Truncated ΔPhoU3::Kanamycin cassette with pTH1931 (ptrc); Sm^R, Nm^R	This study
RmP3209	*S. meliloti* RmP110 ΔPhoU2::Kanamycin cassette with pTH2888 (ptrc-phoU); Sm^R, Nm^R	This study
RmP3210	*S. meliloti* RmP110 Truncated ΔPhoU3::Kanamycin cassette with pTH2888 (ptrc-phoU); Sm^R, Nm^R	This study
RmP3211	*S. meliloti* RmP110 ΔPhoU1 with pTH1931 (pTrc plasmid); Sm^R, $Spec^R$	This study
Escherichia coli		
DH5α	*endA1 hsdR17 supE44 thi-1 recA1 gyrA96 relA1 Δ(argF-lacZYA)* Ui69 80d*lacZ* M15	Strain Collection
MG1655	Wild-type strain; F- *arcA*-1655 *fnr*-1655	Rao *et al.* (1998)
MT4	MG1655 *phoU*-G29D	Morohoshi *et al.* (2002)
MT29	MG1655 *phoU*-A83T	Morohoshi *et al.* (2002)
MT616	MT607 (pRK600); Cm^R	Strain Collection
MT2006	MG1655 *ΔpitA*::*frt ΔpitB*::*frt ΔphnC*::*frt* Δ(*pstSCAB-phoU*)	Motomura *et al.*

	560::Km^R	(2010)
MT2016	MG1655 *ΔpitA*::*frt ΔpitB*::*frt ΔphnC*::*frt* Δ(*pstSCAB-phoU*) 560::Km^R *ΔphoA*::*frt ΔyjbB*::*frt ΔglpT*::*frt*	Motomura *et al.* (2010)
M842	DH5α (pTH1944); Tc^R	Milunovic B. 2011
M1420	BW25113 (pKD46) pKD46= P_{araB}-λred. Amp^R (note Rep is temperature sensitive; grow at 30^{o}C)	Datsenko and Wanner (2000)
M1449	DH5α (pTH2505); Tc^R	White, Unpublished
M2072	DH5α pTH2887 (pMW119 carrying *S. meliloti* PhoU); Amp^R	This study
M2073	DH5α pTH2888(Ptrc carrying *S. meliloti PhoU*); Spec^R	This study
M2074	DH5α pTH2889 (pUCP30T plasmid carrying *S. meliloti* PhoU ± 300bp); Gm^R	This study
M2075	DH5α pTH2890 (pUCP30T plasmid carrying *S. meliloti* –partial phoB); Gm^R	This study
M2076	M1420 (No pKD46) carrying plasmid pTH2895 (pUCP30T with phoU::kanamycin cassette); Gm^R, Km^R	This study
M2077	DH5α pTH2891 (plasmid pTH1937 carrying insert of sMC02148); Km^R	This study
M2078	M1420 carrying plasmid pTH2896 (pUCP30T with Truncated PhoU::kanamycin cassette); Gm^R, Km^R	This study
M2079	DH5α pTH2892 (Pst Operon plasmid- from PhoR to PhoB); Km^R, Gm^R	This study
M2080	DH5α pTH2893 (pUCP30T + PhoU down); Gm^R	This study
M2081	MT2006+ pTH2892 (Pst Operon); Km^R, Gm^R	This study
M2082	MT2016+ pTH2892 (Pst Operon) ; Km^R, Gm^R	This study
M2083	MG1655+ pTH2892 (Pst Operon) ; Km^R, Gm^R	This study
M2084	MT4-pMW119; Amp^R	This study
M2085	MT4-pMWPhoU; Amp^R	This study
M2086	MT4- pTH2887 (pMW119 carrying *S. meliloti* PhoU); Amp^R	This study
M2087	MT29-pMW119; Amp^R	This study
M2088	MT29-pMWPhoU; Amp^R	This study
M2089	MT29- pTH2887 (pMW119 carrying *S. meliloti* PhoU); Amp^R	This study
M2090	MG1655-pMW119; Amp^R	This study
M2091	MG1655-pMWPhoU; Amp^R	This study
M2092	MG1655- pTH2887 (pMW119 carrying *S. meliloti* PhoU); Amp^R	This study
Plasmids		
pET21a	Cloning vector; Amp^R	Studier et al. (1986)
PKD13	Template plasmid; Amp^R, FRT-flanked Kanamycin cassette	Datsenko & Wanner (2000)
PKD46	Red recombinase expression plasmid; Amp^R, ara-inducible expression, temperature-sensitive replication	Datsenko & Wanner (2000)
pMW119	Cloning vector; Amp^R	Nippon Gene

pMWPHOU	pMW119 containing the *E. coli phoU* gene; Amp^R	Motomura et al. (2011)
Pucp30T	Cloning vector; Gm^R	Schwizer et al. (2003)
pTH1522	Reporter vector containing FRT site; Gm^R	Cowie et al. (2006)
pTH1931	Empty Ptrc plasmid; $Spec^R$	This study
pTH1937	pTH2001 with *SmaI/XhoI* fragment from pTH1360 cont. *nptII* from Tn5 and FRT site; Km^R/Nm^R	Milunovic B. (2011)
pTH1944	*flp* gene in a pBBR MC5-3 derivative with RK2-*tetR-tetA*	Milunovic B. (2011)
pTH2418	PCR1 + PCR2 (ntds: 570657-571588 + ntds: 572240-573078) in pJQ200mp18 plasmid (Used for making unmarked PhoU deletion)	Rahat
pTH2463	*S. meliloti phoU* gene in pET21a (*NdeI* and *NotI*) with PhoU-His F & R primers; Amp^R	Rahat
pTH2505	pRK7813 (flp); Tc^R	White, Unpublished
pTH2887	*S. meliloti phoU* gene in pMW119 (*SphI* and *BamHI*) with PhoU-Forward & Reverse primers; Amp^R	This study
pTH2888	Ptrc plasmid carrying *S. meliloti phoU* gene; $Spec^R$	This study
pTH2889	pUCP30T plasmid containing *S. meliloti phoU* gene flanked by 340bp upstream and 352bp downstream homologous sequence (*KpnI* and *XbaI*) with DelPhoU-F1 and R1 primers; Gm^R	This study
pTH2890	pUCP30T carrying *S. meliloti* –partial *phoB* gene region; Gm^R	This study
pTH2891	Plasmid pTH1937 carrying insert of sMC02148 insert; Km^R	This study
pTH2892	Fusion plasmid of pTH1937 and pTH1522 containing Pst operon-from *S. meliloti* upstream of *phoR* to *phoB*; Km^R, Gm^R	This study
pTH2893	pUCP30T plasmid carrying *S. meliloti phoU* gene (for moving *phoU* downstream); Gm^R	This study
pTH2895	pUCP30T plasmid containing Km-cassette gene from pKD13 plasmid flanked FRT site and by 340bp upstream and 351bp downstream homologous sequence of *S. meliloti phoU* gene; Gm^R	This study
pTH2896	pUCP30T plasmid containing Km-cassette gene inserted within *phoU* gene, generating Truncated PhoU::Km-cassette; Gm^R, Km^R	This study
Primer Sequence		
DelPhoU-F1	5'GGGGTACCTCATCCTGATGGACGAGCCC3'	This study
DelPhoU-R1	5'GCTCTAGAATGATGATCGGCAGGCGCTCC3'	This study
PhoU-Forward	5'ACATGCATGCAACAGCGCGTCTCCCGAGGAAACG3'	This study
PhoU-Reverse	5'CGGGATCCGCGATCTCAGTCCGTCACGGAACCC3'	This study
PhoU-CheckF1	5'CGATCGTGATCGTCACCCAC3'	This study
PhoU-CheckR1	5' ATGAGAAGGTCGGGCAGGCG3'	This study
Km-R-1021	5'GGGCGGTTTTATGGACAGC3'	Perez-Hernandez, Unpublished

PKD13-KanF1	5’TTAAGATCGACCGAGCCATTCAGAACAGCGCGTATCCCGAGGAAACGAATGTGTAGGCTGGAGCTGCTTC3'	This study
PKD13-KanR1	5’CGCCAAAGCGGCCGGAACAAATTCTGCATAGGCCCGGATGCCGGGCGATCATTCCGGGGATCCGTCGACC3’	This study
Ptrc-PhoUF1	5’CCTTAATTAACAGCGCGTCTCCCGAGGAAACG3’	This study
Ptrc-PhoUR2	5’CCTTAATTAACGATCTCAGTCCGTCACGGAACCC3’	This study
PhoU-CheckF1	5’CGATCGTGATCGTCACCCAC3’	This study
PhoU-CheckR1	5’ATGAGAAGGTCGGGCAGGCG3’	This study
Trunc-PKD13F	5’ACCGAGCCATTCAGAACAGCGCGTCTCCCGAGGAAACGAATATGTCTCACGTGTAGGCTGGAGCTGCTTC3’	This study
Trunc-PDK13R	5’CGGAACAAATTCTGCATAGGCCCGGATGCCGGGCGATCTCAGTCCGTCACATTCCGGGGATCCGTCGACC3’	This study
Pst-1937-F	5’CGGAATTCGAGATGGATGCCCTCGTTCC3’	This study
Pst-1937-R	5’GGACTAGTATGGCACTCGACGAAGCACC3’	This study

Table 2: Alkaline phosphatase phenotype of E. coli mutants on agar plates

Strains	No Plasmid	pMW119	pMWphoU	pTH2887
MG1655	White	White	White	White
MT4	Blue	Blue	White	Blue
MT29	Blue	Blue	White	Blue

E. coli MG1655 (wildtype), MT4 (*phoU* mutant) and MT29 (*phoU* mutant) were transformed with pMW119 (empty plasmid), pMWphoU (pMW119 with *E. coli phoU*) and pTH2887 (pMW119 with *S. meliloti phoU*) plasmids and transformants were plated onto LB containing 50µg/ml X-phos. After 24 hours incubation at 37^{o}C, colonies were scored as blue or white.

Table 3: Transfer frequency of the FLP plasmid into *S. meliloti* recipient strains

RmP110, M1449 (pTH2505), MT616			
Media:	**Dilution:**	**Number of Colonies:**	**Frequency:**
LB Sm/Tc	10^{-3} plate	383	1.27×10^{-1}
LB Sm	10^{-5} plate	30	
RmP110, M1449 (pTH2505), MT616			
Media:	**Dilution:**	**Number of Colonies:**	**Frequency:**
LB Sm/Tc (2.5mM PCA)	10^{-3} plate	251	2.28×10^{-1}
LB Sm (2.5mM PCA)	10^{-5} plate	11	
RmP3198, M1449 (pTH2505), MT616			
Media:	**Dilution:**	**Number of Colonies:**	**Frequency:**
LB Sm/Tc	10^{-3} plate	1121	$3.63x\ 10^{-2}$
LB Sm	10^{-5} plate	308	
RmP3198, M1449 (pTH2505), MT616			
Media:	**Dilution:**	**Number of Colonies:**	**Frequency:**
LB Sm/Tc (2.5mM PCA)	10^{-1} plate	9	8.91×10^{-6}
LB Sm (2.5mM PCA)	10^{-5} plate	101	
RmP110, M842 (pTH1944), MT616			
Media:	**Dilution:**	**Number of Colonies:**	**Frequency:**
LB Sm/Tc	10^{-3} plate	105	1.31×10^{-2}
LB Sm	10^{-5} plate	80	
RmP3198, M842 (pTH1944), MT616			
Media:	**Dilution:**	**Number of Colonies:**	**Frequency:**
LB Sm/Tc	10^{0} plate	7	5.6×10^{-7}
LB Sm	10^{-5} plate	125	
RmP3209, M1449 (pTH2505), MT616			
Media:	**Dilution:**	**Number of Colonies:**	**Frequency:**
LB Sm/Tc	10^{-4} plate	134	1.12×10^{-1}
LB Sm	10^{-6} plate	12	
RmP3209, M1449 (pTH2505), MT616			
Media:	**Dilution:**	**Number of Colonies:**	**Frequency:**
LB Sm/Tc (2.5mM PCA)	10^{-3} plate	254	1.41×10^{-2}
LB Sm (2.5mM PCA)	10^{-6} plate	18	

The conjugation frequency of plasmids pTH1944 and pTH2505 carrying FLP-recombinase into RmP110 (wildtype *S. meliloti*) and RmP3198 (*S. meliloti* RmP110 *ΔphoU*::Kanamycin cassette). The conjugation frequency was similar for RmP110 strain with or without induction of pTH2505 with 2.5 mM protocatechuic acid (PCA). The frequency of RmP3198 strain with uninduced and induced pTH2505 is different by factor of 10^4.

Whereas the conjugation frequency using the plasmid pTH1944 that expresses FLP constitutively shows similar frequency to the pTH2505 plasmid induced. The difference in frequency between wildtype and RmP3198 suggests colonies are not viable after induction of FLP mediated deletion in RmP3198. The frequency of RmP3209 strain with uninduced and induced pTH2505 is quite similar, in contrast to RmP3198.

Table 4: Blue/White screening to determine expression of alkaline phosphatase

Strains:	Genotype	Formation of Blue/White colonies on LB media containing X-Phos:	Formation of Blue/White colonies on MOPS 2mM AEp media containing X-Phos:
RmP110	Rm1021 with changed wild-type *pstC*	White	White
RmP2381	RmP110 with pTrc plasmid	White	White
RmP3204	RmP110 with pTH2888 (pTrc*phoU*)	White	White
RmP3197	*S. meliloti ΔphoU*	Blue	Blue
RmP3211	*S. meliloti ΔphoU* with pTrc plasmid	Blue	Blue
RmP3200	*S. meliloti ΔphoU* with pTH2888 (pTrc*phoU)* plasmid	Blue	Blue
RmP3198	*S. meliloti ΔphoU::*Km	White	White
RmP3209	*S. meliloti ΔphoU::*Km with pTH2888 (pTrc*phoU*) plasmid	White	White

This table summarizes formation of blue/white colonies of wildtype *S. meliloti* RmP110, RmP3197, RmP3198 transformed with pTrc plasmid and pTH2888 plasmid on LB and MOPS 2mM AEP media containing 50 ug/ml X-Phos. RmP110 strain formed white colonies in all conditions, where as RmP3197 strain formed blue colonies in all conditions. Colonies were scored after 3 and 6 days of incubation at 30^{o}C for LB and MOPS media respectively.

Bibliography

1. **Roumiantseva ML, Andronov EE, Sharypova LA, Dammann-kalinowski T, Keller M, Young JPW, Simarov B V**. 2002. Diversity of *Sinorhizobium meliloti* from the Central Asian Alfalfa Gene Center **68**:4694–4697.

2. **Ailabilityl A V, Bieleski RL, Division PD, Zealand N**. 1973. Phosphate Pools, Phosphate Transport, and Phosphate Availablility. Annual Review of Plant Physiology. **24:**225-252.

3. **Yuan Z, Zaheer R, Finan TM**. 2006. Regulation and Properties of PstSCAB , a High-Affinity , High-Velocity Phosphate Transport System of *Sinorhizobium meliloti*. Journal of Bacteriology **188**:1089–1102.

4. **Rosenberg H, Gerdes RG, Chegwidden K**. 1977. Two systems for the uptake of phosphate in *Escherichia coli*. Journal of bacteriology **131**:505–11.

5. **Torriani A**. 1990. From cell membrane to nucleotides: the phosphate regulon in *Escherichia coli*. Bioessays. **12:**371-376.

6. **Zaheer R, Morton R, Proudfoot M, Yakunin A, Finan TM**. 2009. Genetic and biochemical properties of an alkaline phosphatase PhoX family protein found in many bacteria. Environmental microbiology **11**:1572–87.

7. **Schweizer H, Boos W**. 1984. Characterization of the *ugp* region containing the genes for the *phoB* dependent sn-glycerol-3-phosphate transport system of *Escherichia coli*. Molecular & general genetics : MGG **197**:161–8.

8. **Wanner BL, Metcalf WW**. 1992. Molecular genetic studies of a 10.9-kb operon in *Escherichia coli* for phosphonate uptake and biodegradation. FEMS microbiology letters **79**:133–9.

9. **Parker GF, Higgins TP, Hawkes T, Robson RL**. 1999. *Rhizobium* (*Sinorhizobium*) *meliloti phn* genes: characterization and identification of their protein products. Journal of bacteriology. **181**:389–95.

10. **Borisova S a, Christman HD, Metcalf MEM, Zulkepli N a, Zhang JK, van der Donk W a, Metcalf WW**. 2011. Genetic and biochemical characterization of a pathway for the degradation of 2-aminoethylphosphonate in *Sinorhizobium meliloti* 1021. The Journal of biological chemistry. **286**:22283–90.

11. **Bardin S, Dan S, Osteras M, Finan TM**. 1996. A phosphate transport system is required for symbiotic nitrogen fixation by *Rhizobium meliloti*. Journal of bacteriology. **178**:4540–7.

12. **Geiger O, Röhrs V, Weissenmayer B, Finan TM, Thomas-Oates JE**. 1999. The regulator gene *phoB* mediates phosphate stress-controlled synthesis of the membrane lipid diacylglyceryl-N,N,N-trimethylhomoserine in *Rhizobium* (*Sinorhizobium*) *meliloti*. Molecular microbiology. **32**:63–73.

13. **Zavaleta-Pastor M, Sohlenkamp C, Gao J-L, Guan Z, Zaheer R, Finan TM, Raetz CRH, López-Lara IM, Geiger O**. 2010. *Sinorhizobium meliloti* phospholipase C required for lipid remodeling during phosphorus limitation. Proceedings of the National Academy of Sciences of the United States of America **107**:302–7.

14. **Voegele RT, Bardin S, Finan TM**. 1997. Characterization of the *Rhizobium* (*Sinorhizobium*) *meliloti* high- and low-affinity phosphate uptake systems. Journal of bacteriology. **179**:7226–32.

15. **Summers ML, Elkins JG, Elliott B a, McDermott TR**. 1998. Expression and regulation of phosphate stress inducible genes in *Sinorhizobium meliloti*. Molecular plant-microbe interactions: MPMI **11**:1094–101.

16. **Bardin SD, Finan TM**. 1998. Regulation of phosphate assimilation in *Rhizobium* (*Sinorhizobium*) *meliloti*. Genetics **148**:1689–700.

17. **Summers ML, Denton MC, McDermott TR**. 1999. Genes coding for phosphotransacetylase and acetate kinase in *Sinorhizobium meliloti* are in an operon that is inducible by phosphate stress and controlled by *phoB*. Journal of bacteriology. **181**:2217–24.

18. **Krol E, Becker a**. 2004. Global transcriptional analysis of the phosphate starvation response in *Sinorhizobium meliloti* strains 1021 and 2011. Molecular genetics and genomics : MGG **272**:1–17.

19. **Yuan Z, Zaheer R, Finan TM**. 2005. Phosphate limitation induces catalase expression in *Sinorhizobium meliloti* , *Pseudomonas aeruginosa* and *Agrobacterium tumefaciens*. Molecular Microbiology. **58**:877–894.

20. **Makino K, Shinagawa H, Amemura M, Kawamoto T, Yamada M, Nakata a**. 1989. Signal transduction in the phosphate regulon of *Escherichia coli* involves phosphotransfer between PhoR and PhoB proteins. Journal of molecular biology. **210**:551–9.

21. **Hulett FM, Lee J, Shi LEI, Sun G, Chesnutt R, Sharkova E, Duggan MF, Kapp N**. 1994. Sequential action of two-component genetic switches regulates the PHO regulon in *Bacillus subtilis.* Journal of Bacteriology. **176:**1348-1358.

22. **Dutta R, Qin L, Inouye M**. 1999. MicroReview Histidine kinases : diversity of domain organization. Molecular Microbiology. **34**:633–640.

23. **Carmany DO, Hollingsworth K, Mccleary WR**. 2003. Genetic and Biochemical Studies of Phosphatase Activity of PhoR **185**:1112–1115.

24. **Makino K, Amemura M, Kim S**. 1998. Mechanism of transcriptional activation of the phosphate regulon in *Escherichia coli*. Journal of Microbiology. 231–238.

25. **Blanco AG, Sola M, Gomis-Rüth FX, Coll M**. 2002. Tandem DNA recognition by PhoB, a two-component signal transduction transcriptional activator. Structure (London, England : 1993) **10**:701–13.

26. **K- E, Makino K, Shinagawa H, Amemura M**. 1986. Nucleotide Sequence of the *phoB* Gene , the Positive Regulatory Gene for the Phosphate Regulon of *Escherichia coli* K-12. Journal of Molecular Biology. **190**:37-44.

27. **Birkey SM, Liu W, Zhang X, Duggan MF, Hulett FM**. 1998. Pho signal transduction network reveals direct transcriptional regulation of one two-component system by another two-component regulator: *Bacillus subtilis* PhoP directly regulates production of ResD. Molecular microbiology **30**:943–53.

28. **Hsieh Y-J, Wanner BL**. 2010. Global regulation by the seven-component Pi signaling system. Current opinion in microbiology **13**:198–203.

29. **Wanner BL**. 1987. Control of phoR-dependent bacterial alkaline phosphatase clonal variation by the phoM region. Journal of bacteriology **169**:900–3.

30. **Wanner BL, Wilmes MR, Young DC**. 1988. Control of bacterial alkaline phosphatase synthesis and variation in an *Escherichia coli* K-12 *phoR* mutant by adenyl cyclase, the cyclic AMP receptor protein, and the *phoM* operon. Journal of bacteriology **170**:1092–102.

31. **Wanner BL, Wilmes-Riesenberg MR**. 1992. Involvement of phosphotransacetylase, acetate kinase, and acetyl phosphate synthesis in control of the phosphate regulon in *Escherichia coli*. Journal of bacteriology **174**:2124–30.

32. **Cariss SJL, Tayler AE, Avison MB**. 2008. Defining the growth conditions and promoter-proximal DNA sequences required for activation of gene expression by CreBC in *Escherichia coli*. Journal of bacteriology. **190**:3930–9.

33. **Kim SK, Wilmes-Riesenberg MR, Wanner BL**. 1996. Involvement of the sensor kinase EnvZ in the in vivo activation of the response-regulator PhoB by acetyl phosphate. Molecular microbiology. **22**:135–47.

34. **Davidson AL, Chen J**. 2004. ATP-binding cassette transporters in bacteria. Annual review of biochemistry **73**:241–68.

35. **Chakraburtty K**. 2001. Translational regulation by ABC systems. Research in microbiology **152**:391–9.

36. **Goosen N, Moolenaar GF**. 2001. Role of ATP hydrolysis by UvrA and UvrB during nucleotide excision repair. Research in microbiology **152**:401–9.

37. **Davidson AL, Dassa E, Orelle C, Chen J**. 2008. Structure, function, and evolution of bacterial ATP-binding cassette systems. Microbiology and molecular biology reviews : MMBR **72**:317–64.

38. **Böhm S, Licht A, Wuttge S, Schneider E, Bordignon E**. 2013. Conformational plasticity of the type I maltose ABC importer. Proceedings of the National Academy of Sciences. **110:**5492-5497.

39. **Jones PM, George a M**. 2004. The ABC transporter structure and mechanism: perspectives on recent research. Cellular and molecular life sciences : CMLS **61**:682–99.

40. **Locher KP**. 2009. Review. Structure and mechanism of ATP-binding cassette transporters. Philosophical transactions of the Royal Society of London. Series B, Biological sciences **364**:239–45.

41. **Chen J, Lu G, Lin J, Davidson AL, Quiocho F a**. 2003. A tweezers-like motion of the ATP-binding cassette dimer in an ABC transport cycle. Molecular cell **12**:651–61.

42. **Deveaux LC, Kadner RJ**. 1985. Transport of Vitamin B12 in *Escherichia coli* : Cloning of the btuCD Region. Journal of Bacteriology. **162:**888-896.

43. **Rao NN, Torriani a**. 1990. Molecular aspects of phosphate transport in Escherichia coli. Molecular microbiology **4**:1083–90.

44. **Qi Y, Kobayashi Y, Hulett FM**. 1997. The pst operon of *Bacillus subtilis* has a phosphate-regulated promoter and is involved in phosphate transport but not in regulation of the pho regulon. Journal of bacteriology **179**:2534–9.

45. **Novak R, Cauwels A, Charpentier E, Tuomanen E**. 1999. Identification of a *Streptococcus pneumoniae* Gene Locus Encoding Proteins of an ABC Phosphate Transporter and a Two-Component Regulatory System. Journal of Bacteriology. **181**:1126-1133.

46. **Ruiz-Lozano JM, Bonfante P**. 1999. Identification of a putative P-transporter operon in the genome of a *Burkholderia* strain living inside the arbuscular mycorrhizal fungus Gigaspora margarita. Journal of bacteriology **181**:4106–9.

47. **Gonin M, Quardokus EM, O'Donnol D, Maddock J, Brun Y V**. 2000. Regulation of stalk elongation by phosphate in *Caulobacter crescentus*. Journal of bacteriology **182**:337–47.

48. **Anba J, Bidaud M, Vasil ML, Lazdunski A**. 1990. Nucleotide sequence of the *Pseudomonas aeruginosa phoB* gene , the regulatory gene for the phosphate regulon. Journal of Bacteriology. **172:**4685-4689.

49. **Filloux a, Bally M, Soscia C, Murgier M, Lazdunski a**. 1988. Phosphate regulation in *Pseudomonas aeruginosa*: cloning of the alkaline phosphatase gene and identification of *phoB*- and *phoR*-like genes. Molecular & general genetics : MGG **212**:510–3.

50. **Wanner BL**. 1993. Gene regulation by phosphate in enteric bacteria. Journal of cellular biochemistry **51**:47–54.

51. **Cox GB, Rosenberg H, Downie J a, Silver S**. 1981. Genetic analysis of mutants affected in the Pst inorganic phosphate transport system. Journal of bacteriology **148**:1–9.

52. **Cox GB, Webb D, Rosenberg H**. 1988. Arg-220 of the PstA protein is required for phosphate transport through the phosphate-specific transport system in *Escherichia coli* but not for alkaline phosphatase repression. Journal of Bacteriology. **170:**2283-2286.

53. **Cox GB, Webb D, Rosenberg H**. 1989. Specific amino acid residues in both the PstB and PstC proteins are required for phosphate transport by the *Escherichia coli* Pst System. American Society of Microbiology. **171:** 1531-1534.

54. **Shi L, Hulett FM**. 1999. The cytoplasmic kinase domain of PhoR is sufficient for the low phosphate-inducible expression of pho regulon genes in *Bacillus subtilis*. Molecular microbiology **31**:211–22.

55. **Rice CD, Pollard JE, Lewis ZT, McCleary WR**. 2009. Employment of a promoter-swapping technique shows that PhoU modulates the activity of the $PstSCAB_2$ ABC transporter in *Escherichia coli*. Applied and environmental microbiology **75**:573–82.

56. **Wykoff DD, O'Shea EK**. 2001. Phosphate transport and sensing in *Saccharomyces cerevisiae*. Genetics **159**:1491–9.

57. **Pratt JR, Mouillon J, Lagerstedt JO, Pattison-granberg J, Lundh KI, Persson BL**. 2004. Effects of Methylphosphonate, a Phosphate Analogu , on the Expression and Degradation of the High-Affinity Phosphate Transporter Pho84 , in *Saccharomyces cerevisiae*. Biochemistry. **43:**14444–14453.

58. **Takemaru K, Mizuno M, Kobayashi Y**. 1996. A *Bacillus subtilis* gene cluster similar to the *Escherichia coli* phosphate-specific transport (*pst*) operon: evidence for a tandemly arranged *pstB* gene. Microbiology. **142**:2017–2020.

59. **Barbe V, Cruveiller S, Kunst F, Lenoble P, Meurice G, Sekowska A, Vallenet D, Wang T, Moszer I, Médigue C, Danchin A**. 2009. From a consortium sequence to a unified sequence: the *Bacillus subtilis* 168 reference genome a decade later. Microbiology. **155**:1758–75.

60. **Sun G, Birkey SM, Hulett FM**. 1996. Three two-component signal-transduction systems interact for Pho regulation in *Bacillus subtilis*. Molecular microbiology **19**:941–8.

61. **Steed PM, Wanner BL**. 1993. Use of the *rep* technique for allele replacement to construct mutants with deletions of the *pstSCAB-phoU* operon: evidence of a new role for the PhoU protein in the phosphate regulon. Journal of bacteriology **175**:6797–809.

62. **Muda M, Rao NN, Torriani a**. 1992. Role of PhoU in phosphate transport and alkaline phosphatase regulation. Journal of bacteriology **174**:8057–64.

63. **Baek JH, Kang YJ, Lee SY**. 2007. Transcript and protein level analyses of the interactions among PhoB, PhoR, PhoU and CreC in response to phosphate starvation in *Escherichia coli*. FEMS microbiology letters **277**:254–9.

64. **Oganesyan V, Oganesyan N, Adams PD, Jancarik J, Yokota HA, Kim R, Kim S**. 2005. Crystal Structure of the " PhoU-Like " Phosphate Uptake Regulator from *Aquifex aeolicus.* Journal of bacteriology. **187**:4238–4244.

65. **Liu J, Lou Y, Yokota H, Adams PD, Kim R, Kim S-H**. 2005. Crystal structure of a PhoU protein homologue: a new class of metalloprotein containing multinuclear iron clusters. The Journal of biological chemistry **280**:15960–6.

66. **Cowie A, Cheng J, Sibley CD, Fong Y, Zaheer R, Patten CL, Morton RM, Golding GB, Finan TM**. 2006. An integrated approach to functional genomics: construction of a novel reporter gene fusion library for *Sinorhizobium meliloti*. Applied and environmental microbiology. **72**:7156–67.

67. **Morohoshi T, Maruo T, Shirai Y, Kato J, Ikeda T, Takiguchi N, Ohtake H, Kuroda A**. 2002. Accumulation of Inorganic Polyphosphate in *phoU* Mutants of *Escherichia coli* and *Synechocystis sp* . Strain PCC6803. Applied and Environmental Microbiology. **68**:4107–4110.

68. **Datsenko K a, Wanner BL**. 2000. One-step inactivation of chromosomal genes in *Escherichia coli* K-12 using PCR products. Proceedings of the National Academy of Sciences of the United States of America **97**:6640–5.

69. **Sadowski PD**. 1995. Cleavage-dependent Ligation by the FLP Recombinase: Characterization of a mutant FLP protein with an alteration in a catalytic amino acid. Journal of Biological Chemistry. **270**:23044–23054.

70. **Richardson JS, Carpena X, Switala J, Perez-Luque R, Donald LJ, Loewen PC, Oresnik IJ**. 2008. RhaU of *Rhizobium leguminosarum* is a rhamnose mutarotase. Journal of bacteriology **190**:2903–10.

71. **Quandt J, Hynes MF**. 1993. Versatile suicide vectors which allow direct selection for gene replacement in gram-negative bacteria. Gene **127**:15–21.

72. **Motomura K, Hirota R, Ohnaka N, Okada M, Ikeda T, Morohoshi T, Ohtake H, Kuroda A**. 2011. Overproduction of YjbB reduces the level of polyphosphate in *Escherichia coli*: a hypothetical role of YjbB in phosphate export and polyphosphate accumulation. FEMS microbiology letters **320**:25–32.